THIAGO DE AZEVEDO REIS

HEMOADSORÇÃO COM RESINA DE POLIESTIRENO DIVINILBENZENO PARA PURIFICAÇÃO SANGUÍNEA

BRASÍLIA, 2025

UNIVERSIDADE DE BRASÍLIA

FACULDADE DE CIÊNCIAS DA SAÚDE

PROGRAMA DE PÓS-GRADUAÇÃO EM CIÊNCIAS DA SAÚDE

THIAGO DE AZEVEDO REIS

HEMOADSORÇÃO COM RESINA DE POLIESTIRENO DIVINILBENZENO PARA PURIFICAÇÃO SANGUÍNEA

Dissertação apresentada como requisito parcial para a obtenção do Título de Doutor em Ciências da Saúde pelo Programa de Pós-Graduação em Ciências da Saúde da Universidade de Brasília

Orientador: Prof. Dr. Francisco de Assis Rocha Neves

BRASÍLIA

2025

THIAGO DE AZEVEDO REIS

HEMOADSORÇÃO COM RESINA DE POLIESTIRENO DIVINILBENZENO PARA PURIFICAÇÃO SANGUÍNEA

Dissertação apresentada como requisito parcial para a obtenção do Título de Doutor em Ciências da Saúde pelo Programa de Pós-Graduação em Ciências da Saúde da Universidade de Brasília

Aprovado em dez de novembro de 2025

BANCA EXAMINADORA

Francisco de Assis Rocha Neves (presidente, primeiro membro)

Universidade de Brasília

Claudio Ronco (segundo membro)

Università degli Studi di Padova

Carlos Eduardo Poli de Figueiredo (terceiro membro)

Pontifícia Universidade Católica de Porto Alegre

Miguel Ângelo de Goés Júnior (quarto membro)

Universidade Federal de São Paulo

Eduardo Cantoni Rosa (suplente)

Universidade Federal de São Paulo

1.1.5 AGRADECIMENTOS

Agradeço à CAPES pois tornou viável essa tese de Doutorado, ao Laboratório de Farmacologia Molecular, Faculdade de Ciências da Saúde da Universidade de Brasília e à *Fondazione International Renal Research Institute of Vicenza (IRRIV)*.

"Great spirits have always encoutered violent opposition from mediocre minds"

Albert Einstein

1.1.7 Resumo em idioma português

O termo adsorção é definido como o processo no qual moléculas se acumulam na camada superficial interfacial de um sólido. O material sólido é o sorbente, e a substância no estado adsorvido é chamada de adsorbato. Os princípios e mecanismos básicos envolvidos na hemoadsorção incluem dinâmica de fluídos, características químicas de materiais sintéticos, isotermas de adsorção, zona de transferência de massa e o efeito Vroman. O desenvolvimento de dispositivos e materiais para hemoadsorção começou na década de 1970, onde carvão ativado revestido em um cartucho de plástico foi usado como sorbente para pacientes com overdose de drogas. Desenvolvimentos posteriores de materiais adsorventes levaram à criação de vários cartuchos, que agora estão disponíveis para uso clínico e são utilizados para uma miríade de propósitos. As indicações para hemoadsorção incluem sepse, intoxicação, overdose de drogas e fármacos, injúria renal aguda, rabdomiólise, síndromes de liberação de citocinas, insuficiência hepática aguda, doenças autoimunes mediadas por anticorpos e uremia. Neste trabalho, descrevo experimentos in vitro e in vivo relacionados à hemoadsorção, especificamente com cartuchos contendo resina de poliestireno-divinilbenzeno. O projeto compreende quatro experimentos in vitro, dos quais três estão publicados, e dois ensaios clínicos, dos quais um está publicado.

1.1.8 Resumo em idioma inglês

Abstract

The term adsorption is defined as the process in which molecules accumulate in the interfacial surface layer of a solid. The solid material is the sorbent, and the substance in the adsorbed state is called adsorbate. The basic principles and mechanisms involved in hemoadsorption include flow dynamics, chemical characteristics of synthetic materials, adsorption isotherms, mass transfer zone, and the Vroman effect. The development of devices and materials for hemoadsorption started in the 1970s, where activated charcoal coated in a plastic case was used as a sorbent for patients with drug overdose. Further developments of adsorbent materials led to the creation of several cartridges, which are

now available for clinical use and are deployed for a myriad of purposes. Indications for hemoadsorption include sepsis, intoxication, drug overdose, acute kidney injury, rhabdomyolysis, cytokine release syndromes, acute liver failure, antibody-mediated auto-immune diseases, and uremia. Herein I describe in vitro and in vivo experiments related with hemoadsorption, specifically with cartridges containing polystyrene-divinylbenzene cartridges. The project comprises four in vitro experiments, of which three are already published, and two clinical trials, of which one is already published.

1.1.10 Lista de Figuras

1.1.11 Lista de Tabelas

1.1.12 Lista de Abreviaturas e Siglas

- AGEs, advanced glycation end products
- AKI, acute kidney injury
- CA-AKI, contrast-associated acute kidney injury
- CKD, chronic kidney disease
- CML, N-carboxymethyllysine
- FiO_2, fraction of inspired oxygen

• HAHDF, hemoadsorption plus hemodiafiltration
• HDF, hemodiafiltration
• HPLC-UV, high-performance liquid chromatography with ultraviolet
• IQR, interquartile range
• PaO_2, partial pressure of oxygen in arterial blood
• $pRR_{(t)}$, partial removal ratio
• RAGE, receptor for advanced glycation end products
• ROS, reactive oxygen species
• RR, reduction ratio
• sRAGE, solubel receptor for advanced glycation end products
• tRR, total removal ratio

1.1.13 Apresentação

During my residency in nephrology (2013 to 2015), I was exposed to continuous renal replacement therapy (CRRT) for critically ill patients. I read with amazement the CRRT handbook, cover to cover, by Professors Bellomo, Kellum, and Ronco. CRRT is an extracorporeal blood purification technique and is the hallmark of nephrointensivism, a sub-specialty representing the intersection between nephrology and intensive care. In 2017, I worked daily with CRRT at the Clínica de Doenças Renais de Brasília (CDRB), lead by Dr. Letícia Reis and Dr. Evandro Reis (my parents). We initiated numerous educational projects in the field. My lectures were full of troubleshooting tips and technical explanations, and I gained national recognition as a key opinion leader in acute kidney injury (AKI) and CRRT. Also in 2017, I attended my first AKI and CRRT course in Vicenza, the most prestigious summit in this field held annually for the past 43 years. The course is organized by my mentor, Professor Claudio Ronco. It was a turning point in my career; I met the renowned researchers in the field in person.

My educational projects were intense, both in the AKI field and also in extracorporeal blood purification therapies for maintenance hemodialysis patients. The projects for patients with kidney failure involved hemodiafiltration, expanded hemodialysis, and short-frequent dialysis. In 2019, I had the opportunity to visit the International Renal Research Institute of Vicenza (IRRIV) for a 10-day period and accepted Professor Ronco's invitation to spend 8 months as a research fellow. Before moving to Italy, I had my first peer-reviewed paper published, a review on AKI. Finally, Thiago Reis was in PubMed. In

parallel, we conducted the first clinical trial at the CDRB for patients undergoing maintenance short-frequent hemodialysis using medium cutoff membranes.

My stay in Vicenza began in January 2020. Shortly after, Italy was severely hit by the pandemic. We were the first to publish on the use of extracorporeal blood purification with hemoadsorption for patients with severe presentation of SARS-CoV-2 infections. Fortunately, top-tier journals published our works, including Nature Reviews Nephrology, Lancet Respiratory Medicine, and Blood Purification. These publications reached Professor Francisco Neves, and we started a collaboration.

In December 2020, we performed the inaugural treatment in Brazil's history using hemoadsorption with styrene-divinylbenzene cartridges in a COVID-19 patient. In 2021, Professor Neves invited me to start a doctoral project about extracorporeal blood purification, focused on critically ill and maintenance hemodialysis patients. Professor Neves was the Head of the Laboratory of Molecular Pharmacology at the University of Brasília. Therefore, my PhD thesis was conducted in this Department and at the university where I graduated with a degree in medicine.

In 2023, I returned to IRRIV for 3 months and we carried out in vitro experiments. Professor Neves visited the research center and participated in the experiments led by Professor Ronco. In 2024, we were the first to perform hemoadsorption for patients receiving online hemodiafiltration in Brazil, and we conducted a clinical trial, also part of this thesis. We are currently collaborating with Professor Fatima Vattimo from the University of São Paulo School of Nursing, where we are conducting in vitro hemoadsorption experiments. Finally, I am currently affiliated with the Laboratory of Medical Investigations 29 (LIM-29) at the University of São Paulo School of Medicine and the Division of Nephrology, under the supervision and leadership of Professor Irene L. Noronha, Full Professor of Nephrology, who sees great value in the innovative field of extracorporeal blood purification and supports research initiatives. Our projects involve undergraduate students, Ph.D., and M.Sc. candidates across different disciplines, aiming to build future independent scientists and original thinkers.

SUMÁRIO

Preface

This thesis covers in vitro and clinical uses of hemoadsorption. The introduction exposes the reader to the rationale and the chemical nature of the adsorption processes and the biological consequences associated with the therapy. Then, it covers the specificities of adsorption processes using styrene-divinylbenzene resin, which is not the only resin used for hemoadsorption; nevertheless, it is the most widely used worldwide. Chapters 1 to 3 present in vitro experiments carried out at the International Renal Research Institute of Vicenza. Chapters 4 and 5 examine clinical trials conducted in patients with kidney failure in Santiago, Chile, and São Paulo, Brazil. Finally, chapter 6 covers an in vitro experiment conducted at the Nursing School of the University of São Paulo.

Introduction

Hemoadsorption is an extracorporeal blood and plasma purification treatment aiming to increase extracorporeal removal of solutes, cells, or pathogens, which, due to their physical-chemical features (e.g., dimension, protein binding, or lipophilicity), are not amenable to diffusive or convective clearance(1). Hemoadsorption represents the dynamic binding of blood-based adsorbates to a solid surface that can remove protein-bound molecules, middle and high-molecular-weight substances, pathogens, and cells. Binding can be transient, prolonged, or reversible depending upon the physicochemical properties of the surface and the conditions of exposure, and may be specific or non-specific. This binding is achieved by blood or plasma flow through a sorbent-containing cartridge(1). In contrast to what happens with dialytic therapies, the removal of molecules by adsorption only requires the contact of blood or plasma with a highly adsorptive biocompatible material. While some hemoadsorption can occur even in the setting of conventional dialytic therapies employing membranes with avid binding properties, the use of beads with very large surface area to mass ratios offers the ability to target more specific molecules or molecular classes and the opportunity to remove greater amounts of such solutes. Moreover, the direct contact with blood and plasma permits the removal of cells and pathogens, and inflammatory molecules(2).

Hemoadsorption has markedly evolved since the initial application close to five decades ago, and enhanced biocompatibility and effective adsorptive membranes have been developed and applied to the treatment of a variety of conditions. Moreover, developments in toxicology, pharmacology, biology, immunology and pathophysiology now provide a rationale for hemoadsorption in patients with poisoning and drug intoxication, sepsis, inflammatory states, and metabolic disorders or endogenous intoxications. However, the evidence is distributed across multiple fields and many aspects remain poorly described and integrated. They include available technologies and physicochemical principles, techniques and modalities, evidence behind possible indications, prescription and monitoring, performance characteristics for different biological and toxicological targets, and the definition of relevant biochemical, biological, physiological, and clinical endpoints(3).

Physicochemical Principles

Chemical adsorption (chemisorption) is a relatively specific, energy-intensive process involving the formation of chemical bonds between the solute and sorbent (relatively uncommon in extracorporeal applications). Physical adsorption is a non-specific process typically mediated by hydrophobic interactions between solute (i.e., adsorbate) and sorbent. Ionic interactions, van der Waal forces and biological affinity binding may also mediate physical adsorption . At any given time, one or more of these mechanisms may be active, and the features of the adsorptive surface, such as surface area, structure, and pore size. In addition, the sorbent configuration represented by bead size and packing density into the cartridge determine the efficiency of adsorption. Solute binding by physical adsorption may occur at high rates due to low energy thresholds. However, such binding is relatively weak (i.e. highly reversible); thus, the rates of desorption, which means the opposite of adsorption, and the displacement by competitive solutes may also be high(4). Such desorption may be a significant drawback of hemoadsorption.

The devices deployed to adsorption are filters or cartridges. In filters, adsorption occurs to blood exposure to membrane-based structure, represented by synthetic hollow fibers packed in a plastic cylinder. Furthermore, in cartridges, blood or plasma interact with porous polymers in form of beads, powder, flakes, granules or a mesh of solid fibers. Irrespective of its form, the sorbent polymer is packed in a plastic cylinder, the hemoadsorption columns. The process of adsorption is based on certain basic principles: (i) a solute reaches the vicinity of the specific binding site by mass transfer, a process impacted by flow rate and fluid phase, that is, solvent characteristics; (ii) the “active” binding area is within the pore structure (pore size is a critical determinant of access to the sorbent); and (iii) once a solute reaches a potential binding site, the likelihood of adsorption and the rate of its occurrence are influenced by factors related to the triad solute, solvent and sorbent(5).

Quantification of Hemoadsorption

From the chemical perspective, adsorptive capacity can be measured in terms of efficacy. For a sorbent cartridge, efficacy can be measured in vitro as mass removal quantified using isotherm equations, elution of the adsorbates and mass transfer zone; and in vitro and in vivo using the removal ratio over time. The isotherm equation curves can be evaluated in vitro as a first step using standard saline solution to assess the affinity of the material for binding specific adsorbates. The removal ratio should also be tested in vitro using saline and blood or plasma to mimic extracorporeal therapies and to study the potential impact of other molecules and cellular elements present in body fluids (5).

From the clinical perspective, the efficacy of adsorption represents the influence of the therapy in clinical outcomes or in biomarkers used as a surrogate. Specific biomarkers may be molecules potentially involved in tissue damage during acute or chronic illnesses. Typical examples of parameters to test the clinical efficacy of hemoadsorption are surrogates, represented by molecular biomarkers such as uremic toxins, cytokines, myoglobin, bilirubin, or medications. Moreover, physiological biomarkers including vascular tonus (e.g., mean arterial pressure) and lung function, [partial pressure of oxygen in arterial blood (PaO_2) divided by fraction of inspired oxygen (FiO_2)]. Examples of clinical outcomes are inotrope-free days, mechanical ventilation-free days, intensive care unit and hospital length of stay, and ultimately, patient survival(6).

Biocompatibility, Biotolerability and Adverse Events

Biocompatibility refers to the capacity of a material or solution to exist in contact with the human body without causing an inappropriate host response(2). The biocompatibility characteristics of adsorptive therapies are like those required for dialysis. Biocompatibility remains an important clinical challenge in both chronic and acute settings due to the spectrum of cellular, humoral and other responses that may be triggered by the interaction of blood with sorbents. Avoiding direct contact between blood and the adsorptive surface through plasma separation may improve system biocompatibility. A more suitable term to describe these interactions may be short-term biotolerability, defined as the ability of a material to reside in the body or have contact to blood for a

certain period of time only with the generation of a low grade and acceptable inflammatory reaction(7).

Measurement of safety parameters includes determination of effects of undesired depletion of endogenous and exogenous substances (i.e. albumin) and cells (i.e. platelets), and unintentional modulation of cell responses and/or biochemical pathways like activation of the coagulation cascade and the complement system and the upregulation of granulocytes, monocytes, lymphocytes, and platelet adhesion molecules(7). A set of molecular markers representing classes of solutes susceptible to adsorption can be used to characterize the safety of hemoadsorption. For example, the systemic effects of hemoadsorption, which can be used to asses safety, include hemodynamic, immunological and metabolic adverse events attributable to the therapy (i.e. anaphylaxis, vasodilation, micronutrient depletion, heparin-induced thrombocytopenic thrombosis, bradykinin release syndrome), depletion of cells and cell products (e.g. leukopenia, anemia, thrombocytopenia, loss of plasma proteins and immunoglobulins), and micronutrient deficiencies(8). A topic of great relevance is the undesirable removal of drugs leading to subtherapeutic concentrations. Examples: i) removal of ticagrelor and apixaban could lead to thrombotic events; ii) removal of anticonvulsants could precipitate seizures; iii) removal of antihypertensives could cause a hypertensive crisis; and iv) removal of antimicrobials could result in pathogen treatment failure(8).

The first symposium on the characterization of porous solids was held in 1987. According to the International Union of Pure and Applied Chemistry classification of pore size, the micropore width is less than 2 nm, the mesopore width is 2 to 50 nm, and the macropore width is above 50 nm. Nowadays, the term nanopore is used to encompass both micropores and mesopores. The rate of movement of fluids into and through porous media is not yet completely understood, and it involves the permeability (or transport resistance) and the morphology of the porous solid(9). Adsorption can result from van der Waals interactions and ionic or hydrophobic bonds(5). Three main steps govern the process of adsorption:

1. Interparticle: the fluid phase (i.e., blood or plasma) perfuses the solid sorbent material within a cartridge, filling the void spaces between the particles or displacing the fluid used to prime the cartridge (**Figure 1a**). The spaces between the particles where the fluid phase permeates are defined as channels.

2. Interphase: the fluid phase flow is tangent to the outer surface of the solid material (**Figure 1b**). On each channel where the fluid phase is dispersed, there is a central region (bulk phase) and a peripherical region, which effectively interacts with the beads.

3. Intraphase: some elements in the fluid phase diffuse into the trabecular interior of the beads through mesopores in the surface of the solid structure (**Figure 1c**).

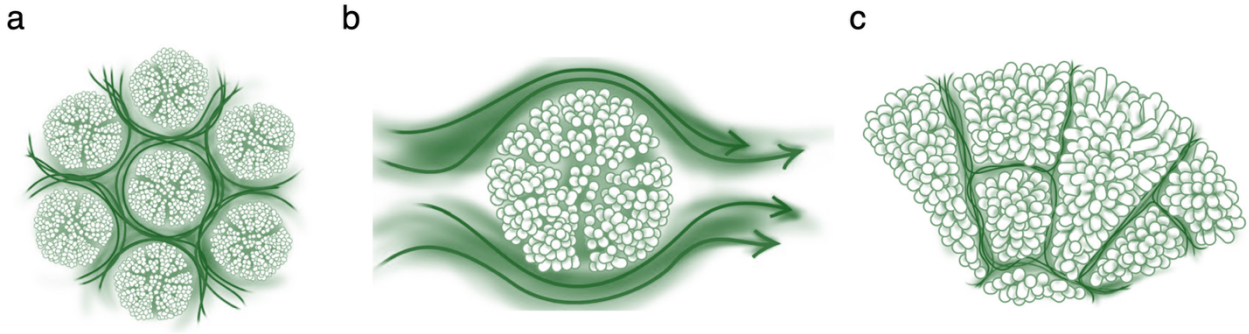

Figure 1. Flow patterns in cartridges with polystyrene-divinylbenzene porous beads. *a Interparticle: first the fluid phase (blood or plasma) permeates the spaces between the beads, creating the so-called channels. b Interphase: the second level of interaction in which the fluid in the periphery of the stream interacts effectively with the sorbent, whereas the central region (bulk) does not have contact with the sorbent. c Intraphase: the third level of interaction where adsorption effectively occurs. By diffusion, the solvent enters through the beads' pores and perfuses the trabecular structure's tortuous paths. Adapted from ref. 6.*

Isotherms

The isotherm represents the correlation between the concentration of the adsorbate (i.e., the target for adsorption) present in the fluid phase and the percentage of adsorption sites on the solid surface of the sorbent material covered by the adsorbate. In the theoretical model of adsorption, the adsorbate creates a single layer in the sorbent surface. The higher the solute concentration for a fixed amount of sorbent, the higher the

percentage of adsorptive sites occupied. Saturation of the sorbent denotes the point where additional increments in the solute concentration will not further increase the adsorptive area covered by the adsorbate. Adsorption isotherms determine the amount of sorbent required to extract a certain amount of the target solute (**Figure 2**). Isotherms are only measured in controlled settings in laboratory experiments. In contrast, during hemo or plasmadsorption, many substances compete for adsorptive sites, preventing the analysis of isotherms(4),(10).

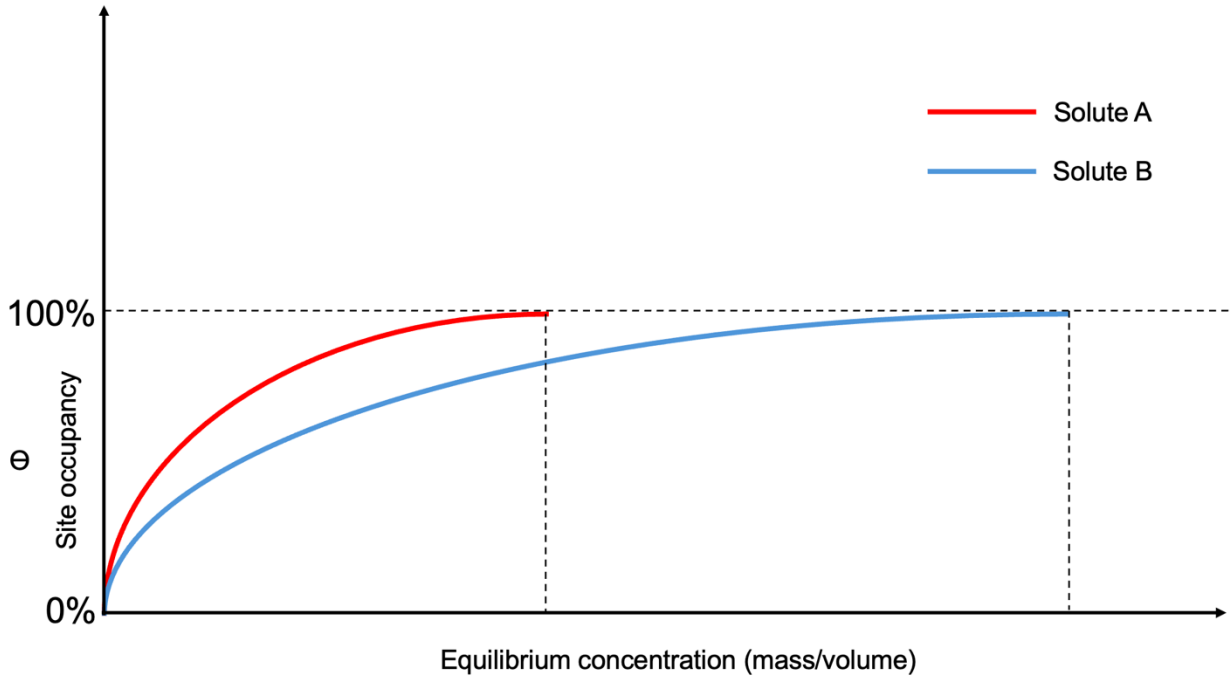

Figure 2. Adsorption isotherms. *In this example, the two curves represent isotherms for different solutes. The maximal sorbent occupancy (Θ) for solute A (red) occurs in a lower concentration than for solute B (blue). Therefore, a higher concentration of solute B is required to saturate the same amount of sorbent.*

Vroman effect

The Vroman effect describes the interactions between proteins and the solid surface of the sorbent material. These interactions may cause conformational changes in the tertiary protein structure. In addition, some proteins might exhibit higher affinity for adsorptive sites and displace proteins with less affinity(11). The properties influencing

protein adsorption are water interaction (hydrophilicity or hydrophobicity), charge, size, and structural stability (**Table 1**).

Table i. Protein and surface properties that affect protein adsorption on material substrates

Proteins	
Property	**Description**
Hydrophilicity/hydrophobicity	Since more hydrophilic side chains are present on the outside of a protein molecule in aqueous media, they may interact with substrate surfaces. Polar (hydrophilic) domains tend to adsorb to polar material surfaces, while hydrophobic domains tend to adsorb to hydrophobic material surfaces
Size	In a multicomponent solution, smaller proteins diffuse more quickly and arrive at the substrate surface faster. Smaller protein, however, form fewer contact points with the material surface than larger proteins
Charge	Charged proteins preferentially adsorb on substrate surfaces of the opposite charge. On most surfaces, however, proteins adsorb the most at their isoeletric point, when the environmental pH is such that the protein has no net charge
Structural stability/rigidity	Proteins that are less structurally stable exhibit greater unfolding upon adsorption onto a material surface and form more contact points/bonds. Proteins that unfold quickly form bonds with the surface before other proteins from a multicomponent solution, such as blood or plasma, arrive at that surface
Surface	
Hydrophilicity/hydrophobicity	Hydrophobic surfaces tend to adsorb more proteins, while hydrophilic surfaces tend to resist protein adsorption
Charge	Opposite charges between the surface and protein promote increased protein adsorption, while like charges tend to reduce protein adsorption
Topography	Increased surface roughness and topological features provide increased material surface area for protein adsorption
Chemistry	The chemical composition of a substrate surface dictates the types of bonds between protein and material surface. $–CH_3$ (methyl) is neutral and hydrophobic, binds strongly to IgG; –OH (hydroxyl) is neutral and hydrophilic, presents decreased affinity for plasma proteins; $–NH_2$ (amino) is positive and hydrophilic, has high affinity for fibronectin; –COOH (carboxyl) is negative and hydrophilic, has increased affinity for albumin

Mass transfer zone

The region where the decaying concentration of a solute occurs along the longitudinal span of the cartridge is defined as the mass transfer zone (**Figure 3**). This zone represents the expected region where the removal of a compound takes place because the reduction in its concentration is proportional to the adsorbed mass(12). The formal definition postulates that this zone starts from the region where the solute concentration is 95% of the inlet concentration until the region where the solute concentration is 5% of the inlet concentration(13).

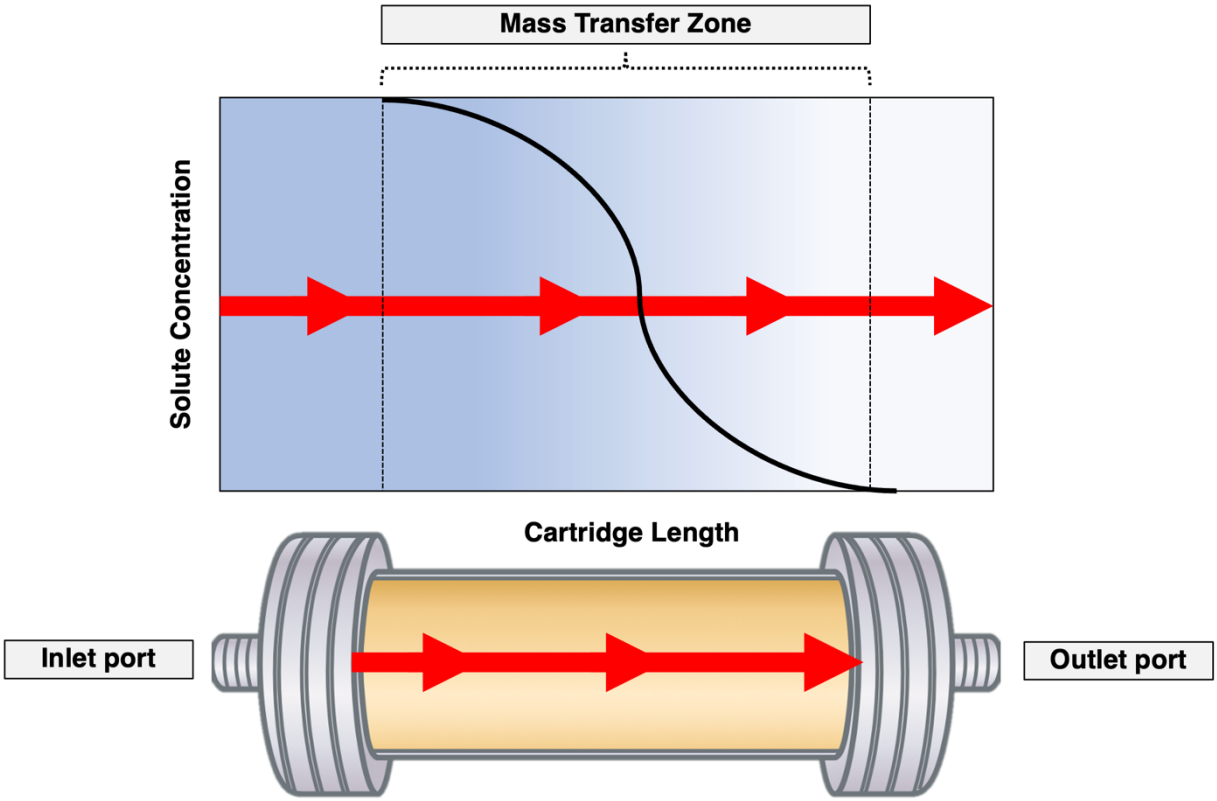

Figure 3. Mass transfer zone (MTZ). *The MTZ is the region that extends along the longitudinal axis of the cartridge. It represents the decay in the solute's concentration during the passage of the solvent through the cartridge. The point at which the solute concentration is indetectable denotes the end of the MTZ. The decay in the solute concentration occurs by its removal through adsorption. The red line with arrows represents the blood flow direction from left to right. The progressive reduction in the background color represents the clearance of the solute from a darker area of the highest concentration toward a lighter area with minimal concentration.*

Current Application and Perspectives

As a closing remark for this initial section, I emphasize that the lack of strong evidence-based knowledge should not preclude the utilization of adsorption-based therapies. Hemoadsorption demonstrates clinically acceptable short-term biocompatibility and safety, as well as technical feasibility. There is also experimental evidence of removal of certain, but no all, molecular targets. Claims that the employment of these treatments should be limited to compassionate fashion or in randomized clinical trials are not fully justified. Many currently applied strategies in many areas of medicine are based on evidence from observational studies, registries, and expert opinion, provided by a solid rationale. Many studies underway show promising results and the use of hemoadsorption in intoxications with protein-bound solutes is already established in clinical practice. Significant progress has been made in the field of extracorporeal blood purification, albeit conclusive evidence to support a routine use of these modalities is lacking. Therefore, these therapies should be individualized to patient-specific needs and resources available. In parallel, further research should be guided by properly designed randomized clinical trials with plausible outcomes.

Chapter 1

Adsorption Mass Transfer Zone of Vancomycin in Cartridges With Styrene-Divinylbenzene Sorbent (12)

Introduction

The polymerization of divinylbenzene produces these synthetic sorbents in the presence of styrene, which functions as a cross-linking agent. The formed copolymer is completely insoluble in the form of porous beads. Its use in extracorporeal blood purification dates back to the 1970s, with AmberLite XAD (DuPont, Willmington, USA) for drug intoxication(14). Currently, these sorbents are used in a vast array of clinical scenarios, including intoxication, cytokine release syndrome from different etiologies, hyperbilirubinemia associated or not with acute liver failure, rhabdomyolysis, and uremia(15),(8),(16),(6),(3),(2). **Table 1.1** shows different cartridges containing styrene-divinylbenzene sorbent used in clinical practice.

Table 1.1. *List of commercially available styrene-divinylbenzene cartridges*

Material	Commercial Name (Manufacturer)	Target of Removal via Adsorption
	Cartridges	
Porous polymer beads – polystyrene divinylbenzene	BS80, BS330, HA60, HA130, HA230, HA330, HA330-II, HA380 and CA330 (Jafron); CytoSorb and DrugSorb (CytoSorbents); MediaSorb (Medtronic); MG150, MG250 and MG350 (Biosun); Plasorba BR-350(L) (Asahi);	Protein-bound compounds, middle molecules, iodinated contrast, drugs, poisons, bilirubin, bile acids, ticagrelor (platelet $P2Y_{12}$ inhibitor), factor Xa inhibitors, organophosphates, paraquat, myoglobin

The first analysis of flow distribution in styrene-divinylbenzene cartridges was carried out in the 1990s, using the in vitro technique developed by Ronco and coworkers(17). In this technique, a cartridge is placed into a computed tomography scan machine and perfused with a solution at different flows. An iodinated contrast media is injected into the inlet line of the circuit and flow distribution is analyzed by sequential images. Flow velocity (cm/s) is higher in the central region when compared to the peripheral region. However, this difference is minimal, and the perfusion of the beads is homogenous(17). In the 2010s, the abovementioned group analyzed other cartridges and observed a different

pattern of flow velocity, where peripheral flow velocity was higher in the periphery when compared to the central region. Again, these differences were minimal(18). An undesired pattern of flow distribution is the channeling phenomenon. In this condition, not all sorbent surfaces are exposed to the fluid because the flow between the beads is not uniform. Therefore, some beads are more permeated than others. This negative feature was not observed in different bead-containing commercially available cartridges tested(17),(18). In addition, the channeling effect can be prevented by choosing a cartridge packing density between 40% to 60%. Packing density is the ratio between the volume occupied by the beads and the recipient's volume, that is, the cylindrical cartridge(19).

Another property explored in these in vitro experiments is the pressure drop, which is the difference between the pressure in the inlet port versus the pressure in the outlet port of the cartridge. A linear positive correlation exists between blood flow and pressure drop, spanning from roughly 20 to 100 mm Hg, with blood flows of 100 to 400 mL/min, respectively. Additionally, pressure drop increases in lengthier cartridges(18).

Material and Methods

Study Desing

The authors carried out an *in vitro* experimental study emulating an extracorporeal circuit applied for hemoadsorption. The study aimed to determine the mass transfer zone of a commercial adsorption cartridge. The elements in the circuit were a blood tubing circuit for hemodialysis, a peristaltic pump, and a modified cartridge packed with sorbent resin. The cartridge was interposed in the circuit downstream of the peristaltic pump. A solution containing vancomycin was propelled into the circuit in a single-pass fashion. The solution samples were collected in four different regions of the cartridge simultaneously. We performed the experiment twice.

Circuit

The circuit was connected to the GALILEO machine (IRRIV Foundation, Vicenza, Italy), in which a peristaltic pump for human hemoadsorption therapy propels the solution, see **Figure 1.1.**

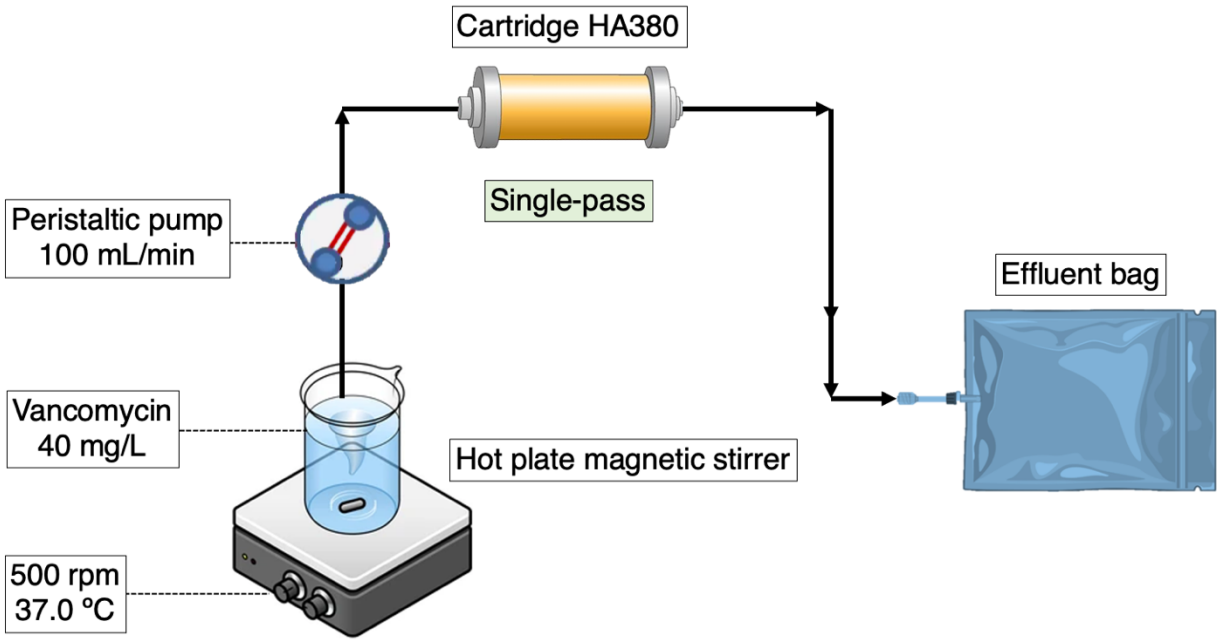

Figure 1.1. Experimental circuit setup. *A peristaltic pump propels a saline solution containing vancomycin from a reservoir through an HA380-modified cartridge in a single-pass fashion. The fluid is collected in an effluent bag.*

A 1,000 mL glass reservoir (Schoot 1000 DURAN; Sigma-Aldrich, Darmstadt, Germany) with a stir bar contained the solution. The reservoir remained over a hotplate magnetic stirrer (VELP Scientifica S.r.l., Usmate Velate, Italy). A blood tubing system for hemodialysis (ArtiSet, Gambro Dasco S.p.A., Medolla, Italy) had its inlet extremity connected to the reservoir and the outlet extremity connected to an effluent bag (MEDICA S.p.A., Medolla, Italy). The modified cartridge was connected downstream of the pump and was held in an upward position, with the inlet port facing downward. The circuit was primed with saline solution.

Modified Cartridge

The authors utilized an HA380 cartridge (Jafron Biomedical, Zhuhai City, China). Table 1.2 describes the device specifications.

Table 1.2. *Device technical data.*

Adsorbent material	Double crosslinked styrene-divinylbenzene copolymers
Mean pore size	3.34 nm
Mean bead diameter	~800 µm
Cartridge volume	400 mL
Adsorbent volume‡	380 mL
Priming volume‡	150 mL
Housing material	Polycarbonate
Mesh (net rack)	Polyester
O-ring seals	Silicone
Blood flow range	100 - 700 mL/min
Effective adsorption area	54.000 - 60.000 m^2
Sterilization	Gamma irradiation
Manufacturer	Jafron
Commercial name	HA380

‡Information provided by the manufacturer.

The cartridge contains sorbent resin (double crosslinked styrene-divinylbenzene copolymers) in the form of porous beads with an average diameter of 800 µm. The housing (cylinder) of polycarbonate has 19 cm on its longitudinal axis (considering the caps) and 6 cm in diameter, a total volume of 400 mL, and a priming volume of 150 mL (when already filled with the resin). The cartridge was empied, the resin discarded, four holes were drilled 3 cm apart from each other in the longitudinal axis, and a 200 cm intravenous administration tubing system (Three stop, Aries S.r.l., Mirandola, Italy) was inserted into each hole. The tip of the line was located in the inner part of the cylinder, as depicted in **Figure 1.2**.

Figure 1.2. Modified cartridge. *The images in the left and in the middle show the modified cartridge emptied. The tip of the tubes was positioned in the center of the polycarbonate cylinder. The image on the right demonstrates the cartridge filled with sorbent material with a spherical shape (beads), and the position where the tube perforates the cylinder.*

The priming volume of the line was 1.6 mL. On the day of the experiment, all the resin from a new cartridge was transferred to the modified one.

Vancomycin Sampling and Measurement

Vancomycin (Zengac, Fisiopharma S.r.l., Palomonte, Italy) was added to a 3,000 mL bag and dissolved in a 0.9% NaCl solution (Na 154 mmol/L), up to a concentration of 40 mg/L. The solution was transferred to three glass reservoirs, each containing 1,000 mL, and pumped at 100 mL/min at a constant temperature of 37.0°C. The 3 mL aliquots were obtained after 4 minutes to ensure that the saline priming solution (~150 mL) contained in the cartridge was displaced by the vancomycin solution. In the second experiment, we collected additional samples at 14 minutes in all sites to explore if partial sorbent saturation could influence the mass transfer zone. After each collection, a syringe filled with air was connected to the lines, and 3 mL was pushed into each site. The airflow

forced the remaining solution in the line to return to the circuit. The sampling sites were identified as S0, upstream of the cartridge; S1, S2, S3, and S4, distancing 3, 6, 9, and 12 cm from the inlet port, respectively (**Figure 1.3**).

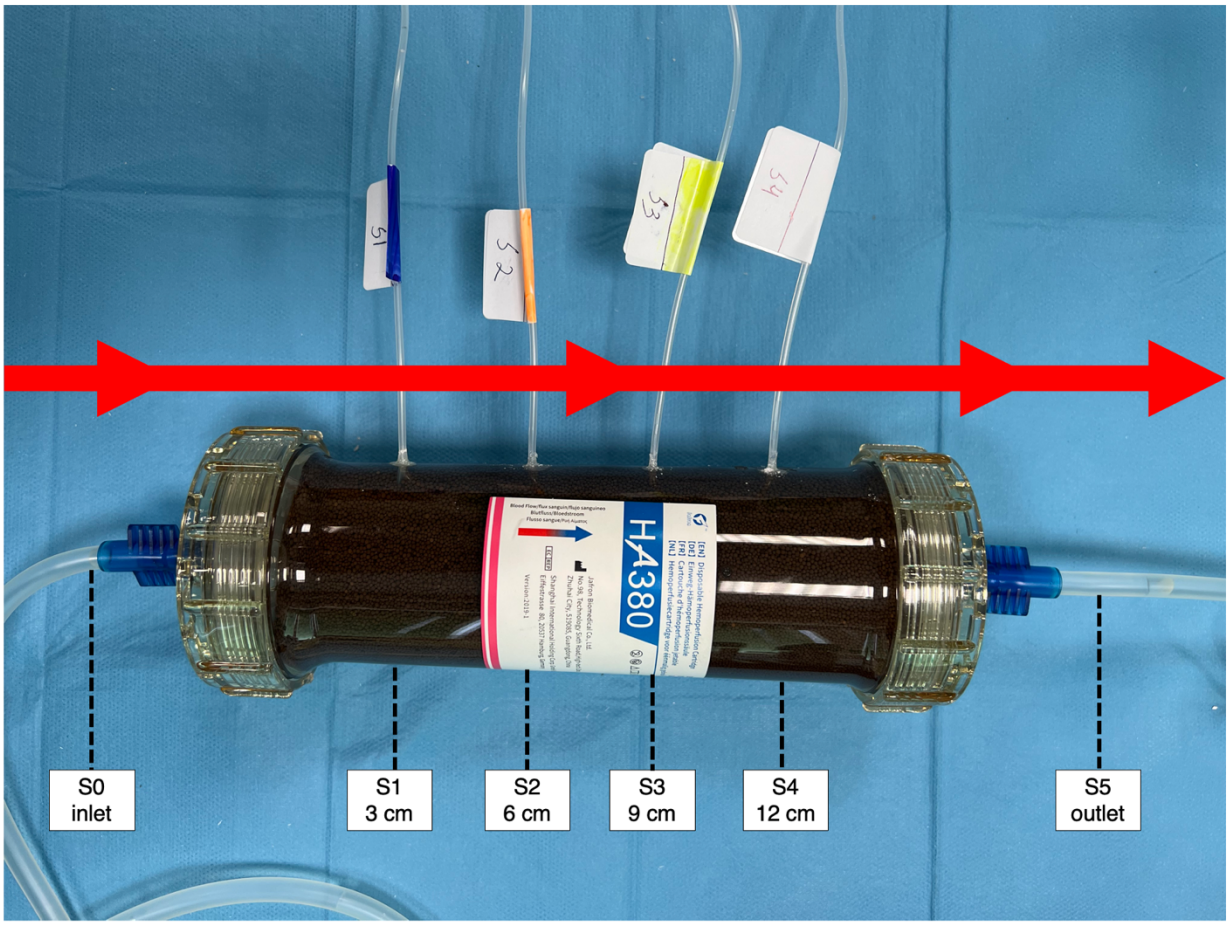

Figure 1.3. Representation of the modified cartridge and the sites to obtain aliquots of the solution. *The sites S0 and S5 are not shown in this image and were represented by the boxes pre- and post-cartridge regions. The red line with arrows represents the solvent flow direction from left to right.*

The S5 site was placed downstream of the outlet port. In both experiments, we measured vancomycin concentration in the effluent bag at the end of the experiment.

The samples were immediately analyzed using a turbidimetric immunoassay method (QMS assay [Thermo Fisher Scientific, Waltham, MA]), in the ILab 650 platform

(Instrumentation Laboratory, Werfen, Bedford, MA). The experiment was terminated after all the 3,000 mL of the vancomycin solution passed through the cartridge, allowing the calculation of the total vancomycin mass adsorbed. This volume was drained into an effluent bag. Because the solution flow was 100 mL/min, the time to collect all the solution in the effluent bag was 30 minutes.

Parameters and Calculations

a) Calculation of single-pass solute clearance (mL/min) is obtained with the following formula:

(1)

$$Vancomycin\ clearance = \frac{(C_{inlet} - C_{outlet}) \bullet Q_S}{C_{inlet}}$$

where C_{inlet} (mg/L) is the pre-cartridge vancomycin concentration, C_{oulet} (mg/L) is the post-cartridge vancomycin concentration, and Q_S is the solution flow (mL/min).

b) Total vancomycin mass adsorbed is measured with the following formula:

(2)

$$i)\ Mass\ adsorbed = Vanco_{initial} - Vanco_{final}$$

where $Vanco_{initial}$ is the total vancomycin mass added into the initial 3,000 mL bag, and $Vanco_{final}$ is the total vancomycin mass in the effluent bag at the end of the experiment.

(3)

$$ii)\ Vanco_{initial} = C_{initial} \bullet V$$

where $C_{initial}$ is the vancomycin concentration (mg/L) in the initial bag, and V (mL) is the total solution volume.

(4)

$$iii)\ Vanco_{final} = C_{final} \bullet V$$

where C_{final} is the vancomycin concentration (mg/L) in the effluent bag at the end of the experiment.

Data Analysis

Due to the simple design of the experiment, specific statistical analyses were unnecessary. Data were plotted in Excel (Microsoft, Redmond, Washington, USA).

Results

Mass Transfer Zone

In the first experiment, samples were drawn from the cartridge after 4 minutes, while in the second experiment, samples were collected after 4 and 14 minutes. **Figure 1.4** depicts the mass transfer zone in the first and second experiments.

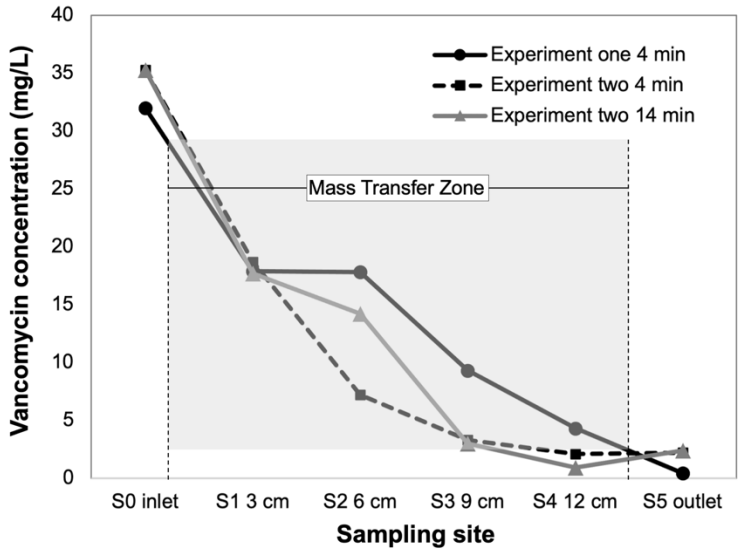

Figure 1.4. Vancomycin mass transfer zone. *The curves demonstrate the reduction in vancomycin concentration along the passage of the solution through the cartridge. The labels in the horizontal axis represent the sampling sites in the circuit (S0 inlet and S5 outlet) and in the cartridge (S1, S2, S3, and S4).*

In the first experiment, the aliquots were drawn simultaneously at minute 4. In the second experiment, the aliquots were drawn at minute 4 and minute 14. The grey zone delimited by the dashed vertical lines represents the mass transfer zone, where the solute concentration ranges from 95% to 5% of the pre-cartridge concentration.

Clearance and Mass Adsorbed

Vancomycin clearance in experiment one at 4 minutes was 98.75 mL/min. In experiment two, the drug clearance at 4 and 14 minutes was 93.76 and 93.2, respectively. An aliquot was drawn from the effluent bag at the end of the experiments to determine vancomycin concentration. In experiment one, the vancomycin total mass was 96 mg, and 92.7 mg were adsorbed, that is, removal of 96.6%. In experiment two, the vancomycin total mass was 105.9 mg, and 97.8 mg were adsorbed, resulting in a removal of 92.3%.

Discussion

The present study demonstrates a strong reduction in vancomycin concentration along the solvent passage through the cartridge. Ideally, all the target compounds should be removed from the liquid phase while passing through the device. When the concentration of a solute in the outlet of a cartridge is still significant, it indicates that not all the solute mass was cleared from the solvent and this situation is termed the flow-through condition(20),(17). The flow-through condition might be a consequence of inadequate cartridge design, insufficient sorbent mass, and sorbent wasting or saturation. In chemical engineering, a packed bed is defined as a hollow vessel filled with a packing material. In our experiment, the former is the polycarbonate cylinder, and the latter is the styrene-divinylbenzene beads(21). The intent of the packed bed is to optimize the interface between the solid surface (adsorber) and the compound in the fluid phase (adsorbate)(22). The HA380 cartridge displays a randomly packed bed structure because the particles (beads) are free to move and relocate in the cylinder.

The flow-through condition might also occur when not all the sorbent surface is exposed to the liquid medium because the interphase flow (i.e., flow in between the

beads) is not uniform, and some regions, represented by a fraction of the beads, are more permeated than others, the so-called channeling effect. We could anticipate channeling is not significant in the HA380 and other commercial cartridges from previous data about fluid dynamics analysis published by our group(17),(18). Channeling effect can also be prevented by choosing a packing density between 40 to 60%. Packing density can be defined as the ratio between the sorbent volume (excluding the volume of the pores) and the volume of the recipient (i.e., the cartridge)(19). For the HA380, the packing density is approximately 60%.

Vancomycin is an antimicrobial member of the glycopeptide drug class. It has a molecular weight of 1,449 Da, and according to the current classification of middle molecules, it is subclassified as a small-middle molecule (molecular weight 500 - 15.000 Da)(23). We have chosen to explore this molecule because of its known adsorption kinetics and affordability for acquisition and analysis. Vancomycin can be used as a surrogate for other middle molecules, such as myoglobin and interleukin 6. Furthermore, we opted for a vancomycin concentration of 40 mg/L because recent consensus guidelines recommend the assessment of peak and trough concentrations of vancomycin, allowing an "area under the curve-guided dosing"(24),(25). It is postulated that a peak concentration of 40 mg/L and a trough concentration of 15-20 mg/L could provide adequate area under the curve for specific pathogens(26). In both experiments, vancomycin single-pass removal surpassed 90%. These findings are clinically meaningful, reinforcing the understanding that dose adjustments of the medications should be a concern in patients undergoing hemoadsorption treatments using styrene-divinylbenzene sorbent. Recently, Furukawa and co-workers published a pre-clinical experiment in sheep measuring the removal of vancomycin and gentamicin with the HA380 cartridge. The authors concluded that an increment of about 30% in the dose of vancomycin is justified for patients undergoing hemoadsorption with this cartridge(27).

Limitations of our study include evaluating one solvent flow (i.e., 100 mL/min), a single baseline solute concentration, only assessing one or two time points, and using saline as the sole solvent. Furthermore, we were not able to attain precisely the desired initial vancomycin concentration. We presume that during the dilution of vancomycin

powder in the glass vial, not all the content was aspirated, explaining the lower-than-expected concentration in the initial bag. Moreover, we collected an additional series of samples at minute 14 only in the second experiment. This variable (i.e., timing of sampling) may be relevant because partial saturation of the sorbent might "shift to the right" the mass transfer zone curve. The influence of other variables such as solvent flow, solute concentration, competitive adsorption in the case of the presence of two or more compounds, progressive saturation of the sorbent, and use of other solvents such as plasma and whole blood warrant further evaluation. Finally, we observed divergence in the reduction of vancomycin concentration in the S2 site (6 cm from the inlet port), **Figure 1.4**. In experiment one, at minute 4, the concentration dropped by 44.8%. In experiment two, at minute 4 and at minute 14, the reduction was 79.6% and 59.8%, respectively. We speculate that the higher reduction at minute 4 in experiment two might have occurred because some beads were inadvertently aspirated and trapped in the line and had more contact with the fluid phase, **Figure 1.5**.

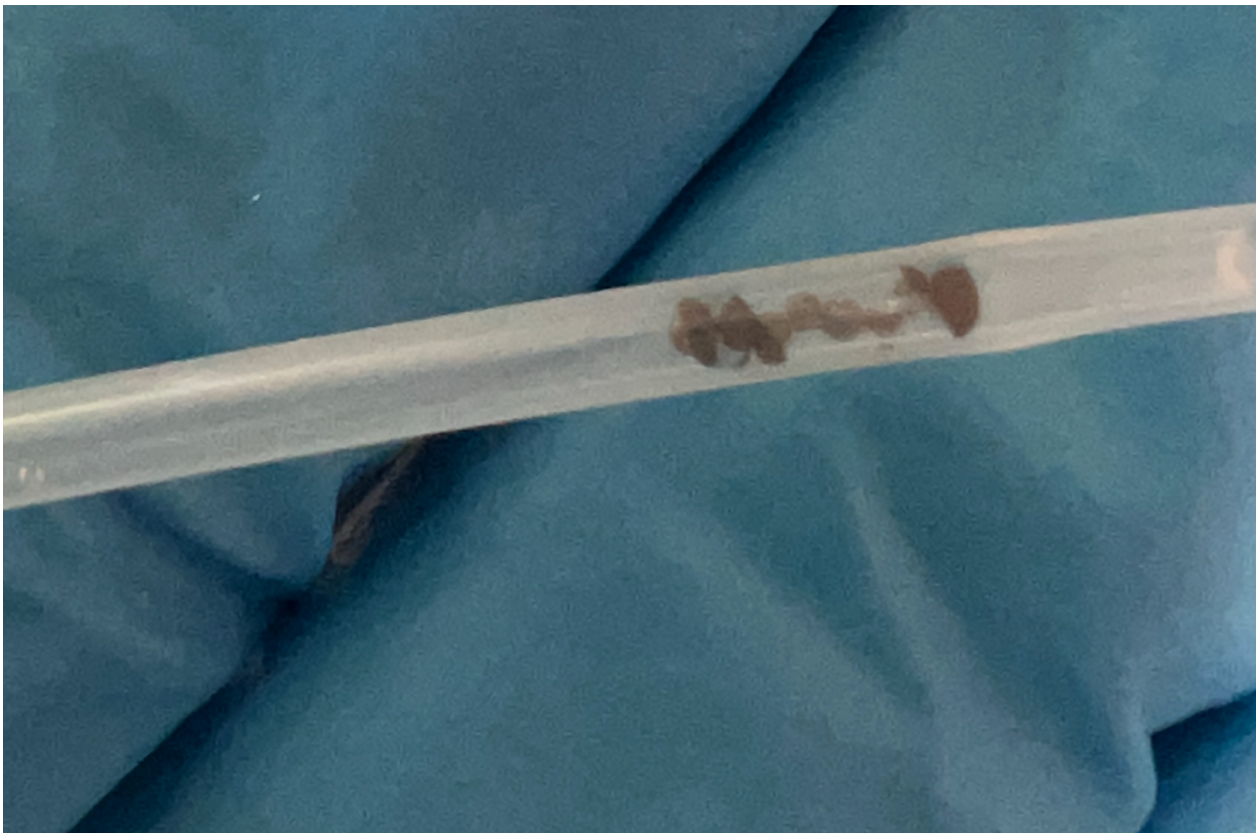

Figure 1.5. Sorbent beads in the sampling lines. *Sorbent beads are trapped inside the line at the S2 site (6 cm from the inlet port). This could increase the contact of the solution passing through the line and the sorbent, falsely increasing the removal of the solute and not necessarily representing the solute concentration inside the cartridge.*

We presume this issue was partially solved in the sampling at minute 14 because the beads observed in the line were flushed back into the cartridge and were not seen in the line. **Figure 1.6** shows the 200 cm plastic tubing intravenous administration system.

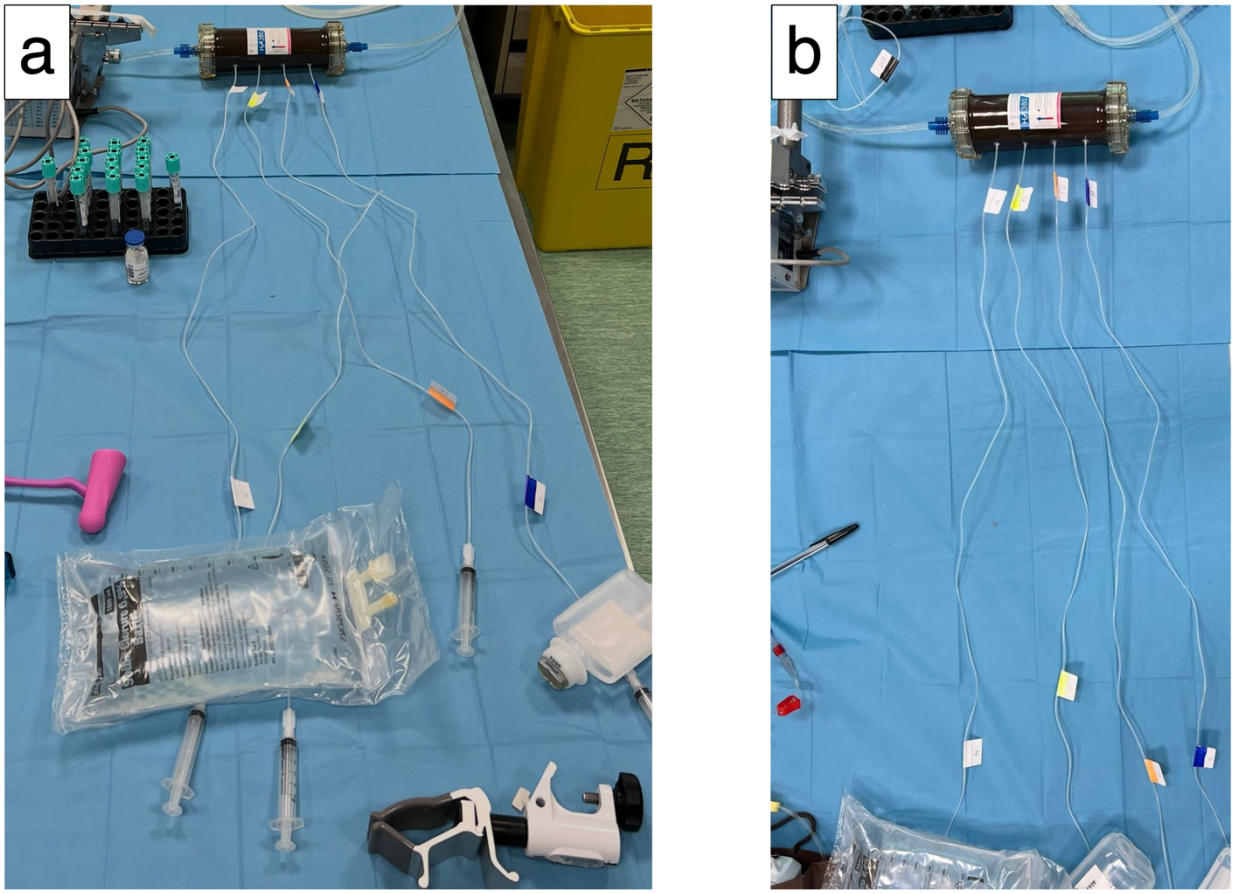

Figure 1.6. Sampling lines. *These are improvised venous lines that were immobilized in the cartridge's side ports. a) Oblique perspective; b) Superior (top down) perspective of the sampling lines..*

Conclusion

Our results point out that the mass transfer zone for a small-middle molecule in a cartridge with styrene-divinylbenzene sorbent covered all the cartridge length and that the adsorption process took full advantage of the cartridge's dimensions. This in vitro study demonstrates that the reduction in the solute concentration occurred progressively, resembling the theoretical sigmoidal shape of the mass transfer zone curve. This implies an adequate and optimal design of the cartridge. In addition, the study of mass transfer zone is crucial for design improvement and further development of cartridges for hemoadsorption.

Chapter 2

Effect of Mechanical Vibration on Kinetics of Solute Adsorption(28)

Introduction

In modern sorbent cartridges, imaging studies have shown negligible local differences in flow velocity at various cross-sectional points of the cartridge due to optimal cartridge design and packing density(18). Peripheral areas of the cartridge characterized by lower bead concentration tend to achieve slightly higher velocities. However, the difference with the bulk flow velocity at the central region of the unit is negligible(18).

Despite flow pattern optimization, further improvements could be theoretically achieved. For example, the application of vibration with different frequencies, amplitudes, and directions might result in beads motion-induced vortices with disruption of preferential flow pathways and channeling. In medical applications, enhanced shear stress induced by vibration can improve plasma exchange efficiency and the ultrafiltration rate in hemofiltration(29). We hypothesized that the presence of these vibration vortices might enhance the contact between blood and beads, promoting a more efficient adsorption of toxins and molecules. The experiment aimed to explore this theory and make a preliminary analysis on the effects of mechanical vibration during hemoadsorption.

Material and Methods

An in vitro model of hemoadsorption to characterize adsorption kinetics with and without vibration of a marker solute was developed. Vancomycin was selected as a marker molecule for this study. The model involves recirculation through an adsorption cartridge a 1,000 mL thermostatic batch of saline solution (37°C) containing 10 g of vancomycin (**Figure 2.1**).

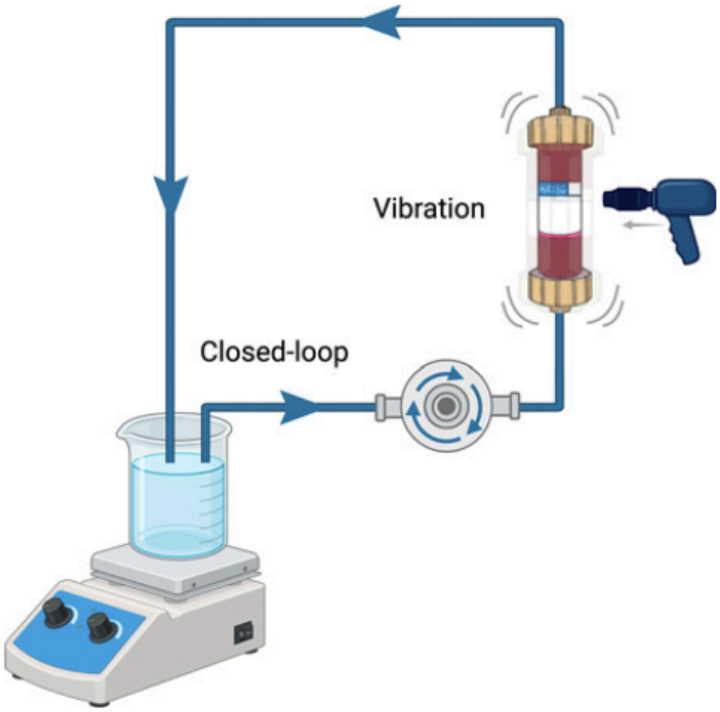

Figure 2.1. In vitro experimental setup. *A customized extracorporeal circuit with the HA380 minimodule is applied to the GALILEO platform. The reservoir is positioned on a magnetic hotplate stirrer.*

This concentration was used due to knowing the kinetics of this vancomycin concentration in a previous study by our group [6]. It was used as a marker molecule and not in a clinical dose. Adequate mixing was ensured by a magnetic hotplate stirrer. A dedicated testing platform (GALILEO) developed in our institute, equipped with flow and pressure sensors and pumps, was used to perform a closed-loop direct hemoadsorption with a minimodule sorbent cartridge (25% of the regular size HA380 cartridge, Jafron, Zuhai, China) containing 75 g of wet neutro-meso/macroporous beads of styrene-divinylbenzene. Different cartridges with the same characteristics were used to perform the experiments with and without vibration. The pore size diameters of the beads are distributed in a wide range of dimensions, allowing the adsorption of solutes between 500 and 60,000 Da. Solute removal is achieved through ionic bonds, van der Waals forces, and hydrophobic bonds. The device was primed according to the instructions for use. Pump flow was set at 250 mL/min, and the duration of the circulation was 120 min. The

vibration model was implemented with a damping head device, with a speed setting at 1,800 percussions per minute, an amplitude of 10 mm, and a frequency of 30 Hz. The vibration device was installed in front of the adsorption cartridge, both in vertical position, targeting the middle segment of the cartridge as the contact area with the percussion head of the vibration device. The direction of flow in the cartridge minimodule was from the bottom to the top. Vancomycin was reconstituted according to the manufacturer´s recommendations and injected into the 1,000 mL saline batch prior to the experiment.

For each study point (0, 10, 30, 90, and 120 min), 3 mL of saline was drawn from the fluid batch container. Each sample was analyzed in triplicate. Vancomycin concentrations were measured using the QMS assay (Thermo Fisher Scientific, Waltham, MA, USA) using the ILab 650 platform (Instrumentation Laboratory, Werfen, Bedford, MA, USA). Removal rate equation was used to calculate the partial removal ratio ($pRR_{(t)}$) of vancomycin at each time point:

$$pRR_{(t)} = (C_0 - C_{(t)}) / C_0$$

where C_0 is the concentration at baseline and $C_{(t)}$ is the concentration at a defined time point.

Total removal ratio was calculated using the formula:

$$tRR = (C_0 - C_{(120)}) / C_0$$

where C_0 is the concentration at baseline and $C_{(120)}$ is the concentration at the end of the experiment (i.e., 120 min).

Two experimental models were carried out, both with a duration of 120 min. The dose of vancomycin, volume of saline solution pump flow, and minimodule cartridge were the same. In the first experiment no vibration was applied (standard), whereas in the second vibration was applied during all the experiment.

Statistical Analysis

The nonparametric Kruskal-Wallis H test was used to compare the results of each time point and different pickup points between the experiments with and without vibration.

A p-value <0.05 was considered statistically significant. The SPSS 25 program ran the analysis.

Results

The $pRR_{(t)}$ at the various time points are reported in **Figure 2.2** for both conditions: vibration and no vibration mode. The $pRR_{(t)}$ at different time points (10 min, 30 min, 60 min, 90 min, and 120 min) were vibration mode 13.8%, 27.6%, 42.1%, 47.4%, 51.4% and standard mode 11.7%, 26.3%, 40.3%, 46.9%, 50%, respectively.

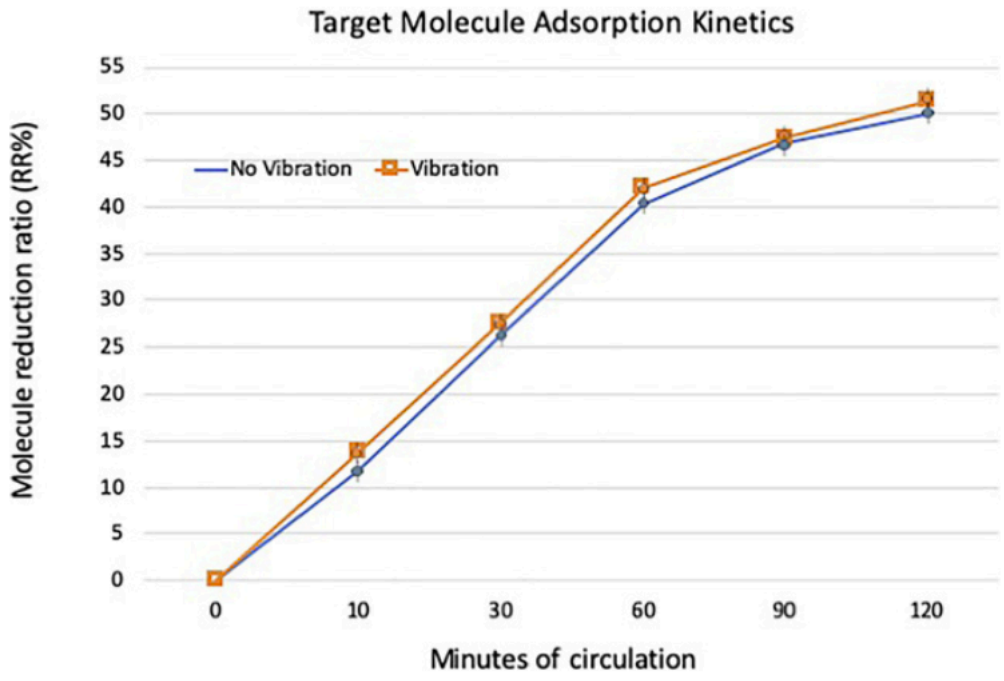

Figure 2.1. Reduction ratios with and without mechanical vibration.

In spite of a slight signal in favor of the vibration mode, adsorption kinetics was statistically not different between the two models (p =0.153). The overall vancomycin adsorbed at 120 min was 5.14 g with vibration and 5.01 g without vibration. The two modalities did not differ significantly in terms of partial reduction ratios, overall amount of adsorbed molecule, or kinetics of adsorption (**Figure 2.2**).

Discussion

Transverse vibration induces a substantial amount of radial mixing in the fluid. It creates a swirling or spiraling motion in the fluid, represented by vorticity contours with the potential beneficial effects of increasing contact time(30). The study question was whether adding mechanical vibration to the unit during a hemoadsorption session could increase both the instantaneous adsorption rate and overall adsorption of the marker molecule. The experiment proved that is this configuration, vibration did not affect adsorption effectiveness. This study has limitations: First, the analysis used saline and not whole blood. In experiments with blood, vibration may reduce the phenomenon of red blood cell packing, enhancing blood flow. Importantly, a downside may be mechanically induced hemolysis. Second, we only explored vancomycin kinetics. Other solutes with different molecular weights and electric potential could behave differently. Third, different vibration frequencies, amplitudes, and vibration directions in comparison with the solution flow (i.e., perpendicular as in the experiment, oblique, or parallel) may affect adsorption effectiveness.

Conclusion

In conclusion, the use of vibration did not affect the removal of vancomycin adsorption with cartridge containing a polystyrene-divinylbenzene resin.

Chapter 3

Iodinated Contrast Adsorption in Cartridges With Styrene-Divinylbenzene Sorbent(31)

Introduction

Contrast-associated acute kidney injury (CA-AKI) is a frequent complication in patients with chronic kidney disease (CKD) receiving intra-arterial iodinated contrast for cardiac procedures such as coronary angiography/angioplasty, ventriculography, and transcatheter aortic valve replacement(32),(33). Up to 14% of patients with CKD stage ≥4 (i.e., estimated glomerular filtration rate <30 mL/min/1.73 m^2) present acute kidney injury (AKI) following these percutaneous procedures(34). Additionally, persistent kidney dysfunction, defined as a sustained reduction in the estimated glomerular filtration rate below 25% of the baseline, occurs in 12% of these high-risk individuals(34). In light of the established deleterious long-term outcomes in the continuum process of AKI, acute kidney disease, and CKD(35),(36), it is logical to investigate interventions to prevent or mitigate CA-AKI. Notwithstanding, to date, pharmacological interventions and hemodialysis have been ineffective in preventing CA-AKI(37),(38). The current recommendations for the prevention or mitigation of CA-AKI comprise the discontinuation of potentially nephrotoxic medications and administration of isotonic intravenous crystalloid prior and following the contrast-enhanced procedure(38).

Kellum and co-workers tested the adsorptive properties of a specific divinylbenzene sorbent for iodinated contrast in two different in vitro models(39),(40). The results of these proof-of-concept experiments were encouraging. Indeed, iodinated contrast was efficiently removed. Nonetheless, an experimental model emulating an extracorporeal circuit in a closed-loop configuration, using commercially available elements (e.g., cartridge, sorbent resin, peristaltic pump, blood tubing), with iodinated contrast doses and solution flow applied in clinical practice, was never built. Therefore, information such as adsorptive efficiency over time after exposure to a commonly used contrast dose, contrast clearance, and sorbent saturation are lacking.

Some studies have demonstrated a dose-response association between the volume of iodinated contrast and CA-AKI in percutaneous cardiac procedures(41),(42). Accordingly, there is biological plausibility in exposing high-risk patients to the smallest possible amount of contrast to prevent CA-AKI. Some strategies are already applied to minimize contrast exposure, such as using biplane angiography to acquire two images for each injection, automated injectors, and thinner catheters (e.g., 4 Fr or 5 Fr). The removal of iodinated contrast by hemoadsorption could be envisioned as an additional tool to reduce the risk of CA-AKI. A conceivable clinical scenario comprises high-risk patients submitted to complex procedures in which a higher contrast volume will likely be required.

We constructed a closed-loop extracorporeal circuit with components and setup parameters used in clinical practice. A cartridge filled with sorbent resin was interposed downstream of a peristaltic pump, and a solution with iohexol was recirculated. The aim of this study was to assess the impact of adsorption on the kinetics of an iodinated contrast medium using a cartridge with sorbent material. We expect that the study results will establish the basis for conducting preclinical and clinical studies exploring whether contrast removal through adsorption can attenuate or prevent CA-AKI.

Materials and Methods

Study Design

The authors carried out an in vitro experimental study emulating an extracorporeal circuit applied for hemoadsorption. The aim of the study was to determine the adsorptive capacity of a styrene-divinylbenzene cartridge for the iodinated contrast medium iohexol. The main variables explored were the solute reduction ratio, solute clearance, and sorbent saturation. The elements in the circuit were a blood tubing circuit for hemodialysis, a peristaltic pump, a glass reservoir, and a cartridge packed with sorbent resin (**Figures 3.1a** and **3.1b**). The cartridge was interposed in the circuit downstream of the peristaltic pump. A solution containing iohexol was propelled into the closed-loop circuit. Samples of the solution were collected from the reservoir at different time points. We performed the experiment twice.

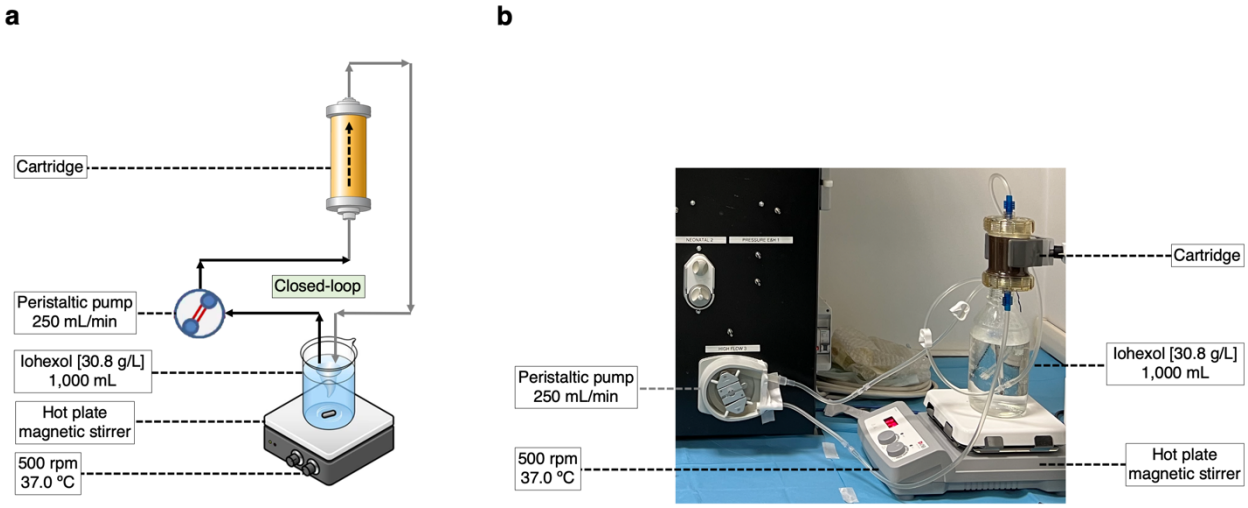

Figure 3.1. Experimental circuit setup. *A peristaltic pump propels a saline solution containing iohexol from a reservoir through a cartridge. This device contains 125 mL (105 g) of mesoporous sorbent resin (double crosslinked styrene-divinylbenzene copolymers) in beads with an average diameter of 800 µm. The circuit emulates an extracorporeal circuit from blood purification in a closed-loop configuration.* ***(a)*** *Schematic graphic representation of the components and parameters configurations.* ***(b)*** *Picture of the components and parameters configurations during the execution of the experiment.*

Iohexol Solution

A 0.9% NaCl solution (Baxter Gambro S.p.A., Medolla, Italy) was spiked with iohexol (OMNIPAQUE™ 350, GE Health Care S.r.l., Milano, Italy), which contains 755 mg of iohexol equivalent to 350 mg of organic iodine per mL. Iohexol - Bis(2,3-dihydroxypropyl)-5-[N-(2,3-dihydroxypropyl)-acetamido]-2,4,6-triiodo-isophthalamide is an iodinated, water-soluble, nonionic monomeric contrast medium (**Figure 3.2a** and **3.2b**).

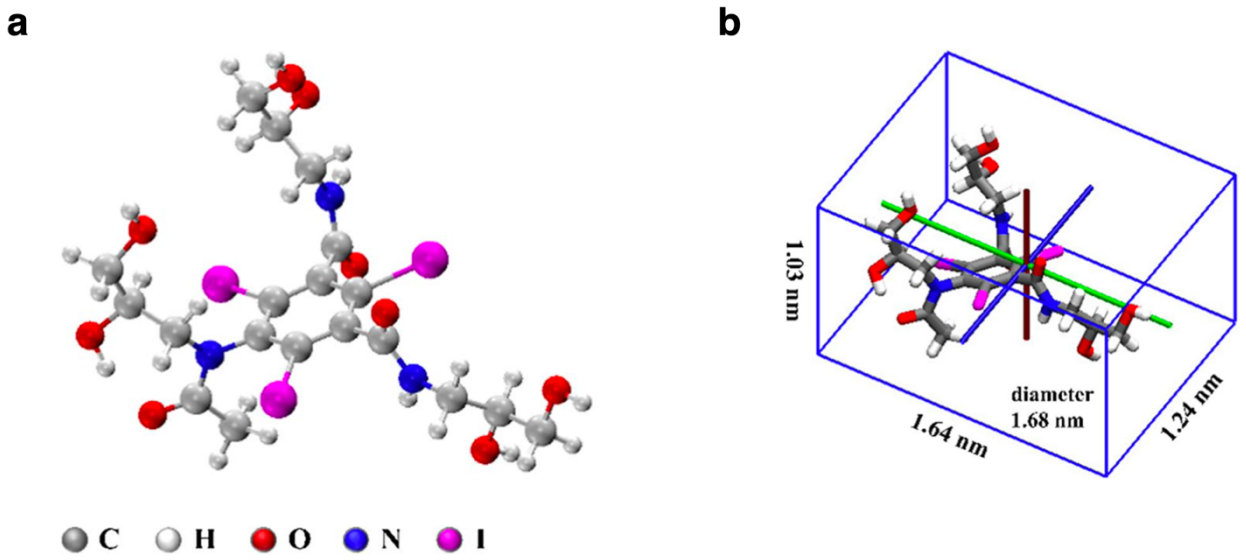

Figure 3.2. Iohexol properties. (a) *Tridimensional molecular structure.* ***(b)*** *Molecular size.*

Iohexol's molecular weight is 821 Da(43), categorized as a small-middle molecule according to the current classification of middle molecules(23).

We prepared a solution with 40 mL of OMNIPAQUE™ 350 dissolved in 960 mL of 0.9% NaCl, aiming for a final iohexol concentration of 30.2 g/L. The authors decided to use the dose of 40 mL because the mean iodinated contrast volume in complex procedures such as selective coronary arteriography combined with ventriculography or during transcatheter aortic valve replacement is around 100 mL(41),(44). Considering that the blood volume of a 70-kg person is 4,200 mL (60 mL/kg of body weight), if the hematocrit is 40%, plasma volume (i.e., 1 – hematocrit) equals 2,520 mL(45). In these conditions, the theoretical concentration of the contrast medium would be similar to the concentration in plasma in clinical settings. The solution was recirculated into the closed-loop circuit for 60 minutes.

Circuit

The circuit was applied to the GALILEO platform (IRRIV Foundation, Vicenza, Italy), in which a peristaltic pump for extracorporeal circulation propels the solution, see **Figures 3.1a** and **3.1b**. A 1,000 mL glass reservoir (Schott 1000 DURAN, Sigma-Aldrich,

Darmstadt, Germany) with a stir bar contained the solution. The reservoir remained over a hotplate magnetic stirrer (VELP Scientifica S.r.l., Usmate Velate, Italy). A customized blood tubing system for the extracorporeal circuit had its inlet and outlet extremities connected to the reservoir. The modified cartridge was connected downstream of the peristaltic pump and was held in an upward position, with the inlet port facing downwards. The circuit was primed with saline solution.

Cartridge

The authors utilized a mini-module cartridge (1:3 scale model) filled with the sorbent resin of the HA380 commercial cartridge (Jafron Biomedical, Zhuhai City, China).(24) The cartridge contains 125 mL (105 g) of mesoporous(25) sorbent resin (double crosslinked styrene-divinylbenzene copolymers) in the form of beads with an average diameter of 800 µm. The cartridge's technical data are described in **Table 3.1**.

Table 3.1. *Device (HA380 minimodule) technical data.*

Adsorbent material	Double crosslinked styrene-divinylbenzene copolymers
Mass	105 g
Adsorbent volume‡	125 mL
Priming volume‡	100 mL
Mean pore size	3.34 nm
Mean bead diameter	~800 µm
Cartridge volume, length, and radius	200 mL, 9 cm, and 2.66 cm
Housing, net rack, end cover, cap nut, and cap material	Polycarbonate
Filter mesh	Polyester
O-ring seals	Silicone
Blood flow range	100 - 700 mL/min
Effective adsorption area	18.000 - 20.000 m^2
Sterilization	Gamma irradiation
Manufacturer	Jafron

‡Information provided by the manufacturer.

Iohexol Sampling and Measurement

The solution was pumped at 250 mL/min at a constant temperature of 37.0 ºC. The sampling of 2 mL aliquots of the solution occurred at eight time points (0, 5, 10, 15, 20, 30, 40 and 60 minutes). The samples were diluted 1:250, and the results were obtained after the correction for the dilutional factor. Dilution was necessary to adjust the results within the linearity range of the ultraviolet-visible detector, preventing its saturation and underestimation of iohexol concentration. The analysis of the samples was performed in duplicate at the Biological Sales Network headquarters in Castellone.

The method for the iohexol concentration measurement was high-performance liquid chromatography with ultraviolet (HPLC-UV) detection(20) using the FloChrom kit (Biological Sales Network - B.S.N., Castellone, Italy). The analytes are separated by

isocratic chromatography. Notably, iohexol has two structural isomers (i.e., endo- and exo-isomers). The test results in the chromatogram comprise two distinguishable peaks representing the endo and exo forms. Therefore, the total concentration is the sum of the isomers' individual concentrations.

Parameters and Calculations

The reduction ratio is derived from the following formula:

(1)

$$RR_{(t)} = \frac{C_i - C_{(t)}}{C_i}$$

where C_i is the initial concentration, $C_{(t)}$ is the concentration at different time points (t), and consequently, $RR_{(t)}$ is the reduction ratio in the specified time points. The formula to calculate the iohexol mass adsorbed ($Mass_{ads}$) was:

(2)

$$Mass_{ads} = C_i \bullet V \bullet RR_{(t)}$$

where C_i is the initial concentration, V is the solution volume and $RR_{(t)}$ is the reduction ratio at different time points (t).

Finally, iohexol clearance was calculated based on this formula:

(3)

$$Clearance\ (mL/min) = \frac{Elimination\ rate\ (g/min)}{Concentration\ (g/mL)}$$

where the elimination rate is the iohexol $Mass_{ads}$ in a time interval. Thus, the clearance can be calculated as:

(4)

$$Clearance_{(t1,\ t2)} = \frac{Mass_{ads\ (t1,\ t2)}}{[C]_{(t1)} \bullet (t2 - t1)}$$

where the clearance between two time points represented as (t1) and (t2) equals the mass adsorbed during this time interval divided by the solute concentration or [C] in (t1) and by the time interval between (t1) and (t2).

Data Analysis

Due to the experiment's simple descriptive design, specific statistical analyses were unnecessary. Data were plotted in Excel (Microsoft, Redmond, Washington, USA).

Results

Reduction Ratio

In experiment 1, after 60 minutes of recirculation, the iohexol concentration measured by HPLC-UV decreased from 30.73 g/L to 14.44 g/L (**Figure 3.3**), with a reduction ratio of 53.0%. In experiment 2, after 60 minutes of recirculation, the iohexol concentration decreased from 30.82 g/L to 14.44 g/L (**Figure 3.3**), with a reduction ratio of 53.1% (**Table 2**).

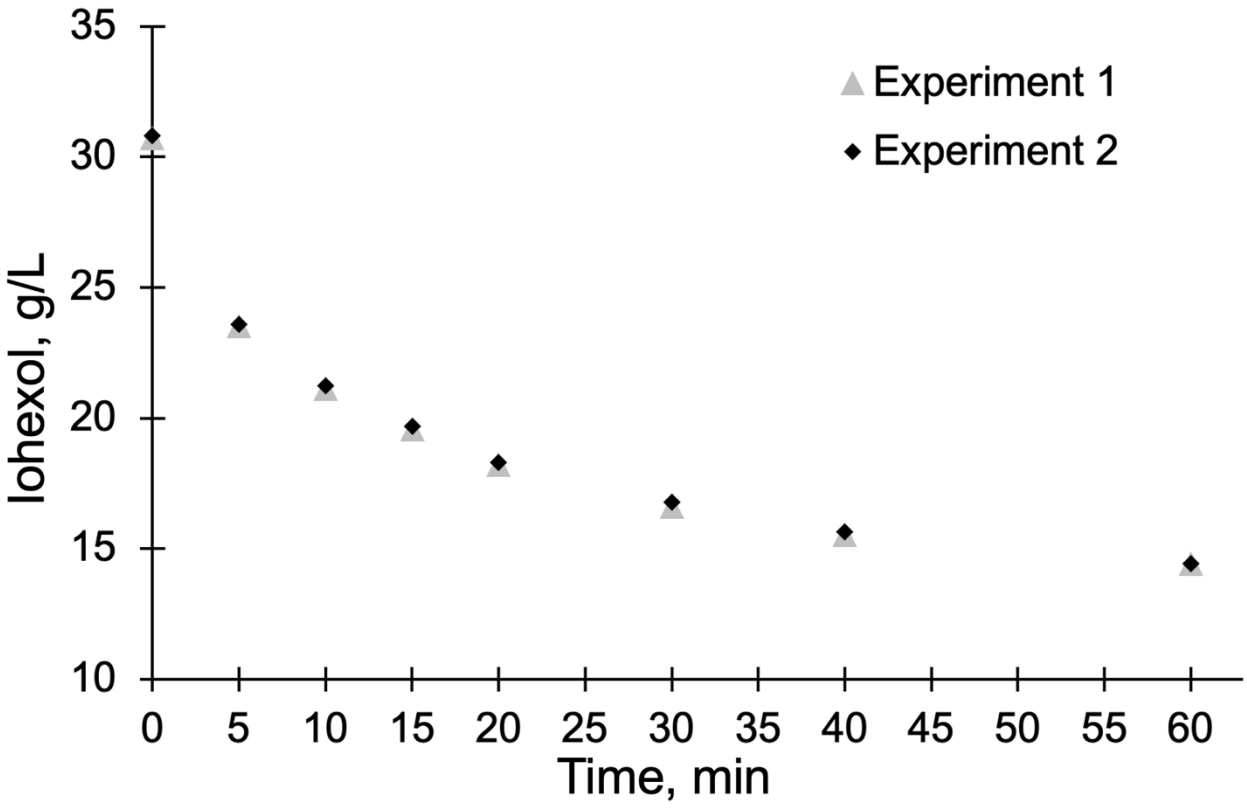

Figure 3.3. Iohexol concentration at defined time points.

Table 3.2. *Iohexol kinetics in an vitro adsorption closed-loop circuit.*

Time (min)	Reservoir (g/L) experiment 1 - mean	Reservoir (g/L) experiment 2 - mean	Reduction ratio (%) experiment 1	Reduction ratio (%) experiment 2	Mass adsorbed (g) experiment 1	Mass adsorbed (g) experiment 2
0	30.73	30.82	–	–	–	–
5	23.54	23.60	23.4	23.4	7.19	7.21
10	21.12	21.23	31.3	31.1	9.62	9.56
15	19.57	19.70	36.3	36.1	11.15	11.13
20	18.21	18.30	40.7	40.6	12.51	12.51
30	16.63	16.78	45.9	45.6	14.10	14.05
40	15.55	15.65	49.4	49.2	15.18	15.16
60	14.44	14.44	53.0	53.1	16.29	16.37

Iohexol Clearance

Iohexol clearance decay over time for both experiments is represented in **Figure 3.4**.

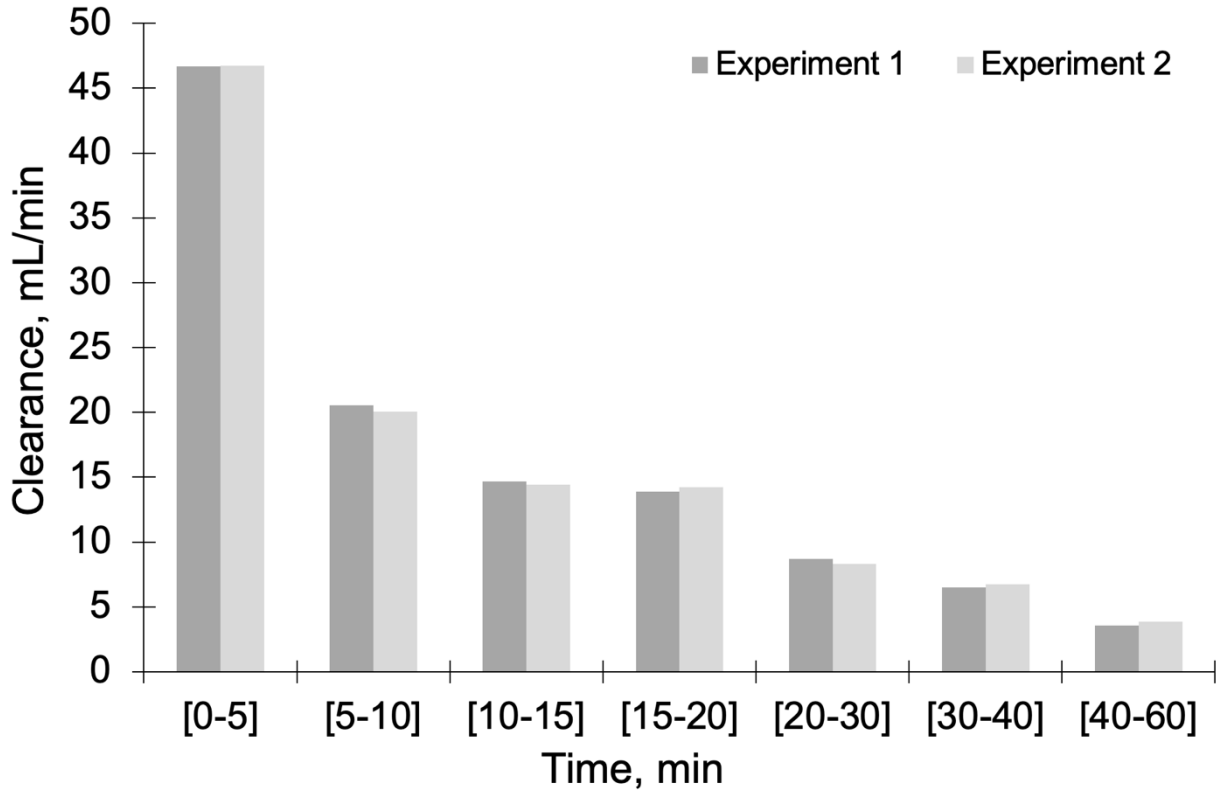

Figure 3.4. Iohexol clearance at the defined time points.

In experiment 1, the iohexol clearance was 46.79 mL/min during the first five minutes, decaying to 3.57 mL/min during the last 20 minutes. Similarly, in experiment 2, the iohexol clearance was 46.72 mL/min during the first five minutes, decaying to 3.87 mL/min during the last 20 minutes (**Table 3.3**).

Table 3.3. *Iohexol clearance by adsorption*

Time (min)	Elimination rate (g/min) experiment 1	Elimination rate (g/min) experiment 2	Clearance (mL/min) experiment 1	Clearance (mL/min) experiment 2
0 – 5	1.438	1.440	46.79	46.72
>5 – 10	0.484	0.474	20.56	20.08
>10 – 15	0.310	0.306	14.68	14.41
>15 – 20	0.272	0.280	13.90	14.21
>20 – 30	0.158	0.152	8.68	8.31
>30 – 40	0.108	0.113	6.49	6.73
>40 – 60	0.056	0.061	3.57	3.87

Sorbent Saturation

In both experiments, after 40 minutes, the reduction in the iohexol concentration was marginal, denoting the sorbent's saturation. At 60 minutes, the total mass adsorbed was 16.29 g and 16.37 g in experiments 1 and 2, respectively (**Table 3.2**). Since each cartridge contained 105 g of sorbent, the ratio of adsorbate/sorbent is approximately 155 mg/g. Therefore, each gram of the sorbent can remove roughly 155 mg of iohexol dissolved in a saline solution at 37.0 ºC.

Discussion

This in vitro study demonstrates that iohexol is efficiently removed from a saline solution via adsorption with a styrene-divinylbenzene resin. The two experiments yielded almost identical results. Approximately half of the total iohexol mass was cleared from the solution during the experiment, which comprised 60 minutes of recirculation. Of note, roughly 50% of the removal occurred during the first five minutes, whereas only about 4% occurred during the last 20 minutes. From a clearance perspective, during the first minutes, the iodinated contrast clearance was 47 mL/min, while it decayed to around 4 mL/min from 40 minutes onwards.

The use of saline as the solvent is a limitation of our study. The presence of other solutes in plasma or whole blood could decrease adsorption efficiency. Therefore, the assessment of efficacy in vitro using saline cannot be extrapolated for the clinical context. Probably, the efficiency in clinical use is not as much as pointed out by our results. This can occur because of competition for adsorptive sites in the resin and unintended protein (e.g., fibrinogen) deposition and pore obstruction in the beads, preventing the interaction between solutes and the sorbent outer and inner surfaces. The pump flow was set at 250 mL/min, impeding explorations related to flow variations. At lower solvent flows, there is more time for interaction between the fluid phase and the sorbent, at the cost of taking a more extended period to circulate all the solution through the cartridge, which can impact the adsorption kinetics. Another independent variable we did not explore was the initial solute concentration. A higher initial concentration may intensify the clearance decay over time.

Our data shows that each gram of resin can adsorb approximately 155 mg of iohexol. The commercially available cartridge HA380 has 310 g of resin. Hence, ~50 g of iohexol

can be adsorbed in this cartridge, equivalent to the amount present in 66 mL of OMNIPAQUE™ 350. In complex procedures such as transcatheter aortic valve replacement, the mean volume of contrast administered is 100 mL(41). This implies that roughly two-thirds of the iohexol mass in this volume could be removed in a 1 to 2-hour hemoadsorption session with the HA380 cartridge before saturation. From a clinical perspective, two consecutive treatments, each using one HA380 cartridge, could enhance contrast elimination and minimize the exposure of body tissues to the contrast medium.

Conclusion

A 1:3 scale model of the HA380 cartridge containing 105 g of styrene-divinylbenzene resin efficiently removes iohexol in an experimental extracorporeal blood purification circuit setup. In proportion, the mass removed would represent roughly two-thirds of the amount administered in major cardiac endovascular interventions. These findings provide a rationale for exploring hemoadsorption as an intervention in clinical trials to prevent or mitigate CA-AKI in high-risk patients.

Chapter 4

Efficacy of HA130 Hemoadsorption in Removing Advanced Glycation End Products in Maintenance Hemodialysis Patients(46)

Introduction

Maintenance hemodialysis patients continue to face a high rate of medium- to long-term complications and frequent hospitalizations. This has resulted in part from the retention and accumulation of uremic toxins with specific effects on inflammation, anemia, osteoarticular and cardiovascular alteration(47),(48). Advanced glycation end products (AGEs) constitute a heterogeneous group of compounds derived from the nonenzymatic glycation of proteins, lipids, and nuclear acids through a complex sequence of Millard reactions(49). At least 20 types of AGEs have been described: N-carboxymethyllysine (CML), pentosidine, and hydroimidazolone are among the best characterized and are markers of AGEs accumulation in several tissues(49).

The accumulation of AGEs in patients with chronic kidney diseases is primarily driven by reduced renal clearance, oxidative stress, and chronic inflammation. These pro-inflammatory and pro-oxidative compounds contribute to endothelial dysfunction and cardiovascular disease by binding to the receptor for advanced glycation end products (RAGE). This interaction activates pathways that increase reactive oxygen species (ROS) levels through NADPH oxidase and mitochondrial dysfunction, as well as induce pro-inflammatory gene transcription, including cytokines like IL-6, IL-1α , and TNF-$\alpha(49)$.

Additionally, soluble forms of RAGE (sRAGE) have been described as generated by either alternative splicing or proteolytic cleavage, acting as decoy receptors and thus exerting a protective function by mitigating the deleterious effects of the activation of the full-length receptor(50). AGEs also cause vascular damage independent of receptors by altering proteins and lipoproteins. Glycation of LDL cholesterol promotes macrophage uptake, leading to foam cell formation and atherosclerosis. Additionally, AGE-modified LDL and matrix proteins like collagen VI disrupt endothelial adhesion and amplify inflammation, exacerbating vascular complications in diabetes and CKD(49).

AGEs represent protein-bound uremic retention solutes, which are poorly eliminated because of their protein-binding characteristics and large molecular weight, particularly in patients who have lost their residual renal function. Dialysis membranes have been developed to remove the protein-bound uremic toxins and reduce mortality in patients living with kidney failure(50). However, the removal rate of AGEs obtained by using hemodialysis or hemodiafiltration is only less than 20% - 32%, and only low-molecular-mass AGEs (<10 kDa AGEs peptide), which may not be able to effectively remove the toxins that are producing rapidly in maintenance hemodialysis patients.

No data is reported on the utilization of HA130 cartridges concerning AGEs removal. Therefore, this study aims to evaluate the efficacy of HA130 hemoadsorption in reducing AGEs and middle molecules in patients undergoing maintenance hemodialysis, compared to high-flux hemodialysis.

Materials and Methods

Study Design and Settings

This prospective, non-randomized, single-center study was conducted at the Dialysis Center of Carlos Van Buren Hospital, Valparaíso, Chile, between July and August 2024. The aim was to evaluate the efficacy of the HA130 hemoadsorption cartridge in reducing AGEs and other middle molecules during high-flux hemodialysis.

Patient Selection

-Inclusion Criteria:

- *Patient aged ≥ 18 years*
- *Stable on conventional high-flux hemodialysis thrice weekly for > 3 months*
- *No residual renal function*

-Exclusion Criteria:

- *Active neoplasia*
- *Hypersensitivity to synthetic hemodialysis membranes*
- *Life expectancy <6 months*

- *Pregnancy*
- *Inability to achieve a blood flow ≥350 mL/min*
- *Refusal to participate*

The patients were assigned to two groups, ensuring a balanced distribution regarding age, gender, and years on dialysis. Baseline clinical data were obtained from hospital registries, including demographic characteristics, causes of renal failure, comorbidities, years on dialysis, blood flow, and session time. None of the patients had residual renal function

Interventions

Patient Groups and Treatments

A total of 20 patients undergoing maintenance hemodialysis for more than three months were included in the study. These patients were divided into two groups: ten patients received one session of high-flux hemodialysis, while the other ten underwent one session of high-flux hemodialysis combined with hemoadsorption using the HA130 cartridge. During all sessions, the blood flow was maintained between 350 and 400 mL/min, with a dialysate flow of 500 mL/min and a session length of 210 to 240 minutes. Net fluid removal was individually tailored according to the clinical needs of each patient.

All patients were treated with a polyethersulfone/polyvinylpyrrolidone dialysis membrane (Clearum^{TM} HS series, Medtronic, Minneapolis, USA), characterized by a K_{UF} of 64 mL/h/mm Hg, polypropylene housing free of bisphenol-A, and an albumin sieving coefficient of 0.004. The hemoadsorption cartridge used in the combined treatment group was the HA130 (Jafron, Zhuhai City, China), a neutral mesoporous resin device containing 130 mL of polystyrene resin beads with a 54% packing density.This design allows the adsorption of solutes with molecular weights between 500 and 40,000 Da(51). The cartridge was primed following the manufacturer´s instructions and installed in a pre-filter position, as shown in **Figure 4.1**. The first dialysis of the week was used to perform the sessions and measure protein-bound uremic toxin reduction. Unfractionated heparin was used as the anticoagulant during all treatments.

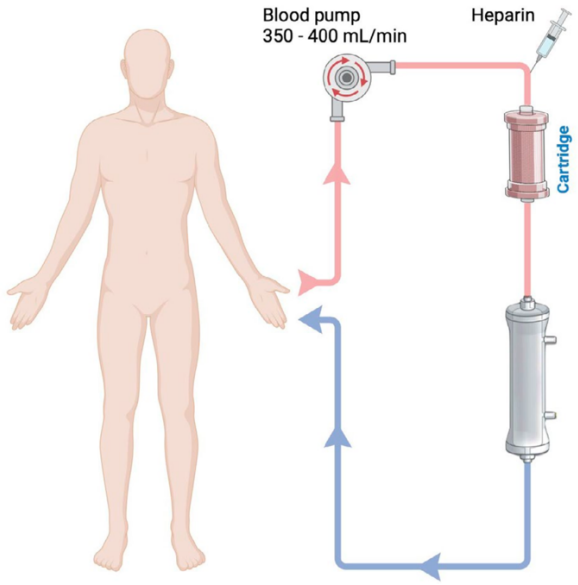

Figure 4.1. Circuit diagram of hemoadsorption plus high-flux hemodialysis.

Blood Sampling and Analysis

Blood samples were collected at the start and end of each session to assess serum levels of carboxymethyllysine, sRAGE, prolactin, ferritin, parathyroid hormone, calcium, phosphorus, bicarbonate, and blood urea nitrogen (BUN). For each time point, 5 mL of blood was drawn using EDTA as an anticoagulant, centrifuged at 1,000 x g for 15 minutes at 2-8°C within 30 minutes of collection, and stored at -20°C until analysis. AGEs concentrations were measured using and ELISA kit at the Biomedical Research Labs, Catholic University of Maule, Talca, Chile.

Calculation of Reduction Ratios

The reduction ratio (RR) of uremic toxins was calculated using the formula:

(1)

$$RR(\%) = 100\ (C_0 - C_{end}) / C_0$$

Where C_0 is the baseline concentration, and C_{end} is the post-treatment concentration.

To account for hemoconcentration, the corrected RR was calculated as follows:

(2)

$$RR_c(\%) = 100\ (C_0 - cC_{end})\ /\ C_0$$

Where:

- $cC_{end} = C_{end} / (1 + [\Delta BW / 0.2\ (BW_{post})])$
- ΔBW = Body weight refers to the change in body weight during the treatment, used to account for variations due to net ultrafiltration.

Statistical Analysis

The data obtained were presented as medians and interquartile ranges for quantitative variables after assessing the normality of the data using the Shapiro-Wilk test. Values of the reduction ratio high-flux hemodialysis plus hemoadsorption were compared with the results obtained with the high-flux hemodialysis group using non-parametric statistical tests. The Chi-square test was used to compare categorical variables, and the Mann-Whitney U test was applied for continuous variables. A value of $p \leq 0.05$ was defined as statistically significant. All analyses were conducted using the SPSS 25 statistical software (SPSS Inc., Chicago, IL, USA).

Ethical Considerations

The San Antonio Valparaíso Health Service Ethics Committee approved this study under resolution 002120, Act No. 61. Informed consent was required for all patients.

Results

The median age was 61.0 years [interquartile range (IQR), 48.0 – 65.0], and 12 patients were male (60%). Eight patients had kidney failure due to diabetic kidney disease (40%), 45% had an undetermined etiology, and 10% had chronic glomerulonephritis. The median time on dialysis was 8.0 years (IQR, 4.8 – 11.0). No adverse events were recorded during the procedures.

The patient's demographic characteristics and laboratory values at the beginning are presented in **Table 4.1**.

Table 4.1. *Demographic and clinical characteristics of the patients.*

	Total	HA + HF-HD	HF-HD	p-value
Age, years	61.0 [48.0 – 65.0]	62.5 [57.3 -72.5]	53.5 [43.8 – 63.3]	0.139
Hypertension % (n)	85.0% (17)	47.1% (8)	52.9% (9)	0.531
Diabetes % (n)	45.0% (9)	55.6% (5)	44.4% (4)	0.653
Heart failure % (n)	50.0% (10)	50.0% (5)	50.0% (5)	1.000
Cardiovascular diseases % (n)	25.0% (5)	60.0% (3)	40.0% (2)	0.606
Blood flow, mL/min	390.0 [350.0 – 400.0]	360.0 [350.0 – 400.0]	400.0 [380.0 – 400.0]	0.142
Dialysis vintage, years	8.0 [4.8 – 11.0]	9.0 [6.5 – 12.5]	6.0 [4.25 – 8.75]	0.287
BUN (pre), mg/dL	64.4 [54.1 – 70.5]	61.9 [52.9 – 69.5]	66.0 [60.0 – 70.1]	0.384
BUN (post), mg/dL	13.5 [11.8 – 17.6]	13.4 [12.9 – 17.2]	13.6 [11.2 – 17.7]	0.929
Ferritin, ng/mL	601.1 [224.4 – 862.5]	538.2 [198.3 – 891.3]	601.1 [366.8 – 807.7]	0.850
Albumin, g/dL	3.8 [3.7 – 3.92]	3.85 [3.7 – 3.9]	3.8 [3.5 – 3.9]	0.969
Bicarbonate, mmol/L	22.0 [19.8 – 23.6]	21.7 [20.1 – 22.5]	22.2 [19.6 – 25.2]	0.437
Calcium, mg/dL	8.8 [8.5 – 9.4]	8.8 [8.4 – 9.4]	8.8 [8.6 – 9.3]	0.819
Phosphorus, mg/dL	4.8 [3.7 – 6.2]	5.2 [4.1 – 6.1]	4.2 [3.2 – 6.1]	0.427

Biochemical parameters did not significantly differ between the treatment groups. The session time of the high-flux hemodialysis plus hemoadsorption group and in the high-flux hemodialysis group was 240 minutes. The median blood flow in the high-flux

hemodialysis plus hemoadsorption group was 360 mL/min (IQR, 350 – 400) mL/min vs 400 mL/min (IQR, 380 – 400) in the high-flux hemodialysis group. No significant differences were observed between groups. The blood flow remained constant throughout the session. All groups utilized dialysate flow of 500 mL/min. Albumin, phosphorus, calcium, ferritin, bicarbonate, and BUN levels were similar at baseline and are shown in **Table 4.1**. Serum prolactin, PTH, CML, and sRAGE levels are presented in **Table 4.2**.

Table 4.2. *Reduction ratios of soluble and protein-bound compounds.*

	HA + HF-HD	HF-HD	p-value
CML (pre), pg/mL	847.3 [722.8 – 1074.4]	956.7 [648.6 – 1009.2]	0.969
CML (post), pg/mL	427.1 [281.2 – 650.6]	612.9 [398.9 – 780.9]	0.472
CML ($post_c$), pg/mL	357.2 [241.6 – 538.3]	539.9 [343.2 – 649.6]	0.473
CML RR	57.5% [45.1 – 70.7]	30.3% [19.1 – 44.5]	0.053
CML RR_c	64.7% [52.6 – 74.9]	39.3% [33.8 – 49.4]	0.045*
sRAGE (pre), pg/mL	3915.8 [2454.2 – 4740.5]	3390.0 [3184.1 – 5915.8]	0.967
sRAGE (post), pg/mL	3249.5 [2331.8 – 3882.4]	3300.2 [2662.2 – 3710.9]	0.965
sRAGE ($post_c$), pg/mL	2839.4 [2035.9 – 3222.9]	2824.9 [2378.8 – 3153.7]	0.896
sRAGE RR	9.8% [0.7 – 18.5]	15.9% [5.9 – 21.2]	0.572
sRAGE RR_c	23.4% [15.1 – 30.4]	21.8 [16.6 – 31.7]	0.791
PTH (pre), pg/mL	782.1 [418.0 – 914.9]	313.5 [121.2 – 761.0]	0.133
PTH (post), pg/mL	507.4 [344.1 – 726.9]	228.3 [33.7 – 574.1]	0.185
PTH ($post_c$), pg/mL	429.6 [293.4 – 660.5]	204.2 [29.9 – 556.4]	0.185
PTH RR	17.7 [15.0-37.4]	34.8 [27.2 – 45.6]	0.216
PTH RR_c	29.8 [24.7 – 44.9]	44.1 [34.9 – 55.4]	0.289
Prolactin (pre), pg/mL	20.4 [13.9 – 23.6]	32.5 [17.3 – 45.7]	0.570
Prolactin (post), ng/mL	11.09 [8.4 – 14.1]	20.1 [11.0 – 26.4]	0.480
Prolactin ($post_c$), ng/mL	9.39 [7.7]	21.7 [13.5 – 32.0]	0.236
Prolactin RR	38.5 [37.6 – 52.0]	36.3 [31.4 – 41.0]	0.167
Prolactin RR_c	47.3 [45.4 – 59.3]	47.7 [36.7 – 51.2]	0.321

Footnote: *p≤0.05; CML, N-carboxymethyllysine; RR, reduction ratio; RR_c, corrected reduction ratio; $post_c$, corrected post; HA, hemoadsorption; HF-HD, high-flux hemodialysis

Baseline levels of the medium-middle molecules prolactin and parathormone were 22.9 ng/mL (IQR, 15.9 – 40.7) and 522.8 pg/mL (IQR, 246.4 – 902.2), respectively. Large-middle molecules baseline level (sRAGE) were 3691.6 pg/mL (IQR, 2464.5 – 5373.4). In relation to protein-bound uremic toxins, the median level of CML was 926.9 pg/mL (IQR, 709.3 – 1042.5).

The reduction ratio was calculated for both the procedures, and results are displayed in **Table 4.2.** Comparing high-flux hemodialysis plus hemoadsorption with high-flux hemodialysis, albumin, phosphorus, calcium, ferritin, bicarbonate, and BUN levels did not shown significant differences between the reduction ratio. A significant reduction of solute levels was only observed for corrected CML 64.7% (IQR, 52.6 – 74.9] vs 39.3% (IQR, 33.8 – 49.4), p =0.045) (**Figure 4.2**). In contrast, no significant differences were observed for this comparison concerning RR and corrected RR of sRAGE, PTH, and prolactin.

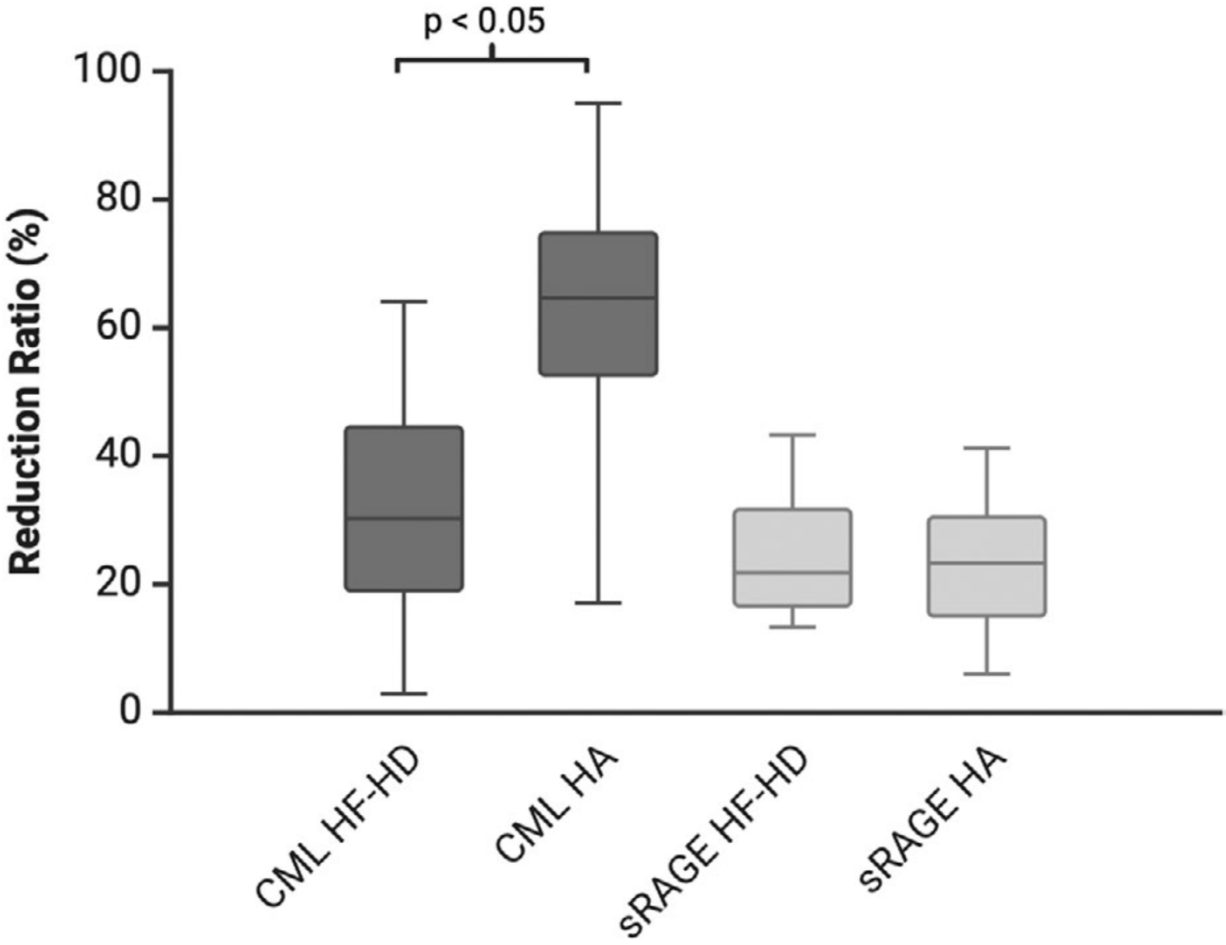

Figure 4.2. Corrected reduction ratios of CML and sRAGE across different treatment modalities. *HF-HD, high-flux hemodialysis; HA, hemoadsorption; CML, N-carboxymethyllysine; sRAGE, soluble advanced glycation end product-specific receptor.*

Discussion

Unlike other studies that primarily focused on uremic toxins, our work targets explicit AGEs, which are increasingly recognized for their role in chronic inflammation and cardiovascular complications in maintenance dialysis patients. Our results demonstrate that the HA130 adsorption cartridge used in the maintenance hemodialysis protocol evaluated in this cross-sectional study significantly enhances the removal of CML, a protein-bound uremic toxin of the AGEs family. A median difference in the reduction ration value of 25.4% was observed comparing the two treatment groups, favouring the hemoadsorption group.

In the context of AGEs accumulation and sorbent materials, only one study reported the utilization of hemoadsorption as a method to reduce AGEs, utilizing a neutral macroporous resin device (MG350) with a diameter of porous about 10 nm. They showed a significant reduction of AGEs (45%-50%) with the combination of hemodialysis with hemoadsorption. In addition, serum levels of AGEs were slowly increased again after switching to the hemodialysis treatment only(52).

Soluble RAGE (constituted by cleaved soluble RAGE form and secreted soluble esRAGE), acts as a scavenger that neutralizes RAGE ligands, promoting protective action by limiting inflammation associated with different diseases(53). Interestingly, sRAGE levels were not significantly reduced in either group. RAGE has a molecular weight of approximately 40 kDa and lacks a transmembrane domain. The size of the pores defined by the cartridges limits the adsorption of this molecule. Preserving sRAGE during hemoadsorption is advantageous, as its reduction could potentially diminish its protective anti-inflammatory role. Maintaining sRAGE levels while enhancing the clearance of pathogenic AGEs like CML highlights the potential to balance efficacy with safety.

Conclusion

The combination of high-flux hemodialysis with hemoadsorption significantly enhances the removal of CML, a deleterious AGEs, without adversely affecting sRAGE levels. This balance between efficacy and safety positions hemoadsorption as a promising adjunctive therapy for kidney failure patients, particularly those at high risk of AGEs-related complications. Further studies are warranted to confirm these findings and explore the long-term benefits of this approach.

Chapter 5

Removal of Middle Molecules With Hemoadsorption plus Hemodiafiltration in Patients With Kidney Failure(54)

Introduction

Hemodiafiltration (HDF) promotes a higher clearance of middle molecules than hemodialysis(55),(56). Whether the association of hemoadsorption plus HDF (HAHDF) using cartridges with styrene-divinylbenzene further enhances the removal of middle molecules is yet to be defined. We prospectively analyzed the removal of middle molecules in four patients undergoing HAHDF (**Figure 5.1**) and compared it with HDF.

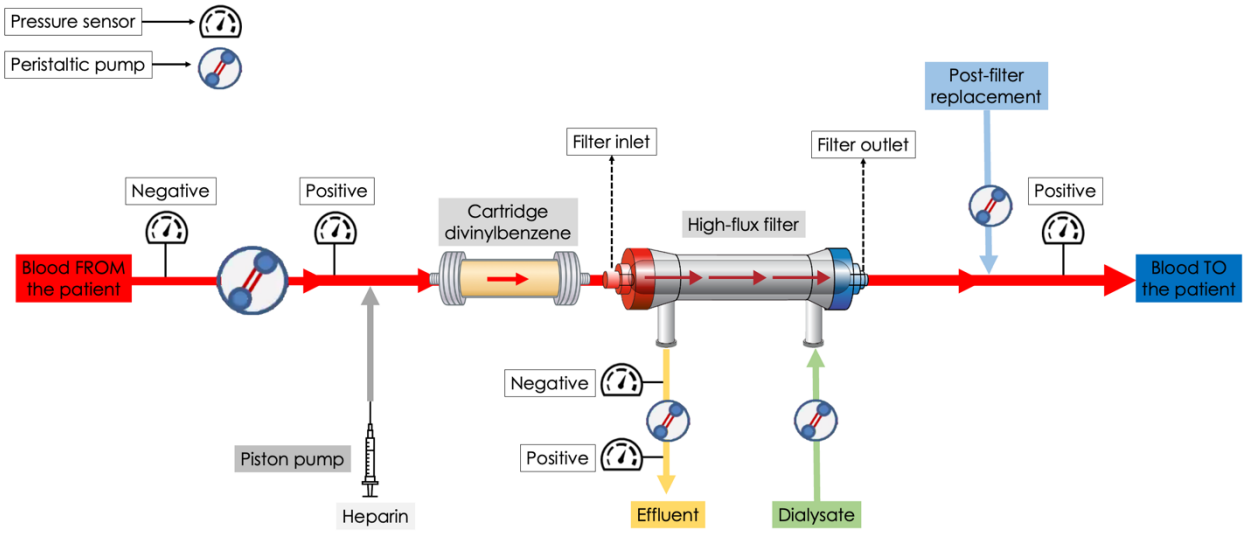

Figure 5.1. Extracorporeal circuit of hemoadsorption plus post-filter replacement hemodiafiltration. *The cartridge is inserted in the upstream of the filter.*

Materials and Methods

Patients underwent 3-hour sessions of HAHDF with post-filter replacement. The extracorporeal circuit setup is depicted in **Figure 5.2a**. In **Figure 5.2b**, the additional blood extension of the blood line is highlighted in g. For each patient, treatment prescription, either HAHDF or HDF, had the same parameters (**Table 5.1**).

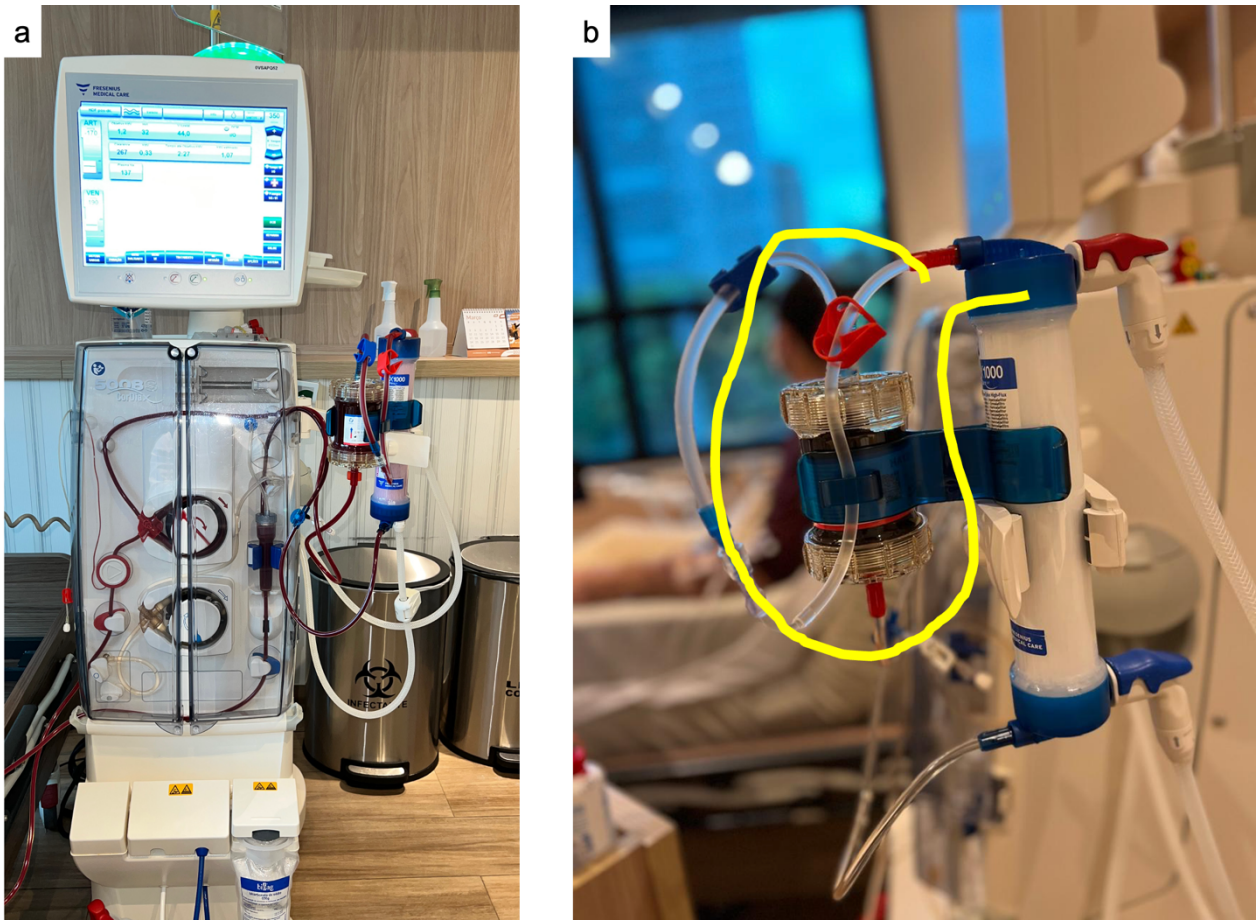

Figure 5.2. Hemoadsorption plus post-filter hemodiafiltration. *a) The picture demonstrates the ongoing therapy utilizing the 5008S machine (Fresenius Medical Care, Bad Hamburg, Germany). b) additional blood line placed after the cartridge to connect it to the high-flux filter.*

Table 5.1. *Main treatment prescritpion variables.*

	Number of HAHDF sessions	Number of HDF sessions	Blood flow (mL/min)	Dialysate flow (mL/min)	Post-filter replacement flow (mL/min)	Vascular access	Filter type/area
Patient 1	8	5	350	500	115	AVF - 15 G needle	Fx CorDiax1000/2.3 m^2
Patient 2	5	5	400	600	115	AVF - 15 G needle	Fx CorDiax1000/2.3 m^2
Patient 3	8	3	400	600	105	AVF - 15 G needle	Fx CorDiax1000/2.3 m^2
Patient 4	8	4	420	500	115	Tunnelled catheter - 14 Fr	Fx CorDiax1000/2.3 m^2

Footnote: AVF, arteriovenous fistula, HAHDF, hemoadsorption plus hemodiafiltration, HDF, hemodiafiltration.

We measured the reduction ratio (RR) [i.e., 1 – (pre-session/post-session)] of four middle molecules in all sessions.

Ethical Considerations

This study was approved by the Federal University of São Paulo – UNIFESP Research Ethics Committee (No. 60256122.0.0000.5505). All participants signed the informed consent.

Results

Four patients performed 29 sessions of HAHDF and 17 sessions of HDF. The main characteristics of the 46 sessions were blood flow of 400 mL/min (IQR, 350-400 mL/min), convective post-filter flow of 115 mL/min (IQR, 105-115), and dialysate flow of 500 mL/min (IQR, 500-600 mL/min). The RR of ß$_2$-microglobulin (12 kDa), myoglobin (17 kDa), and prolactin (23 kDa), were higher with HAHDF. The RR of parathormone (9.4 kDa) was equivalent (**Figure 5.3**).

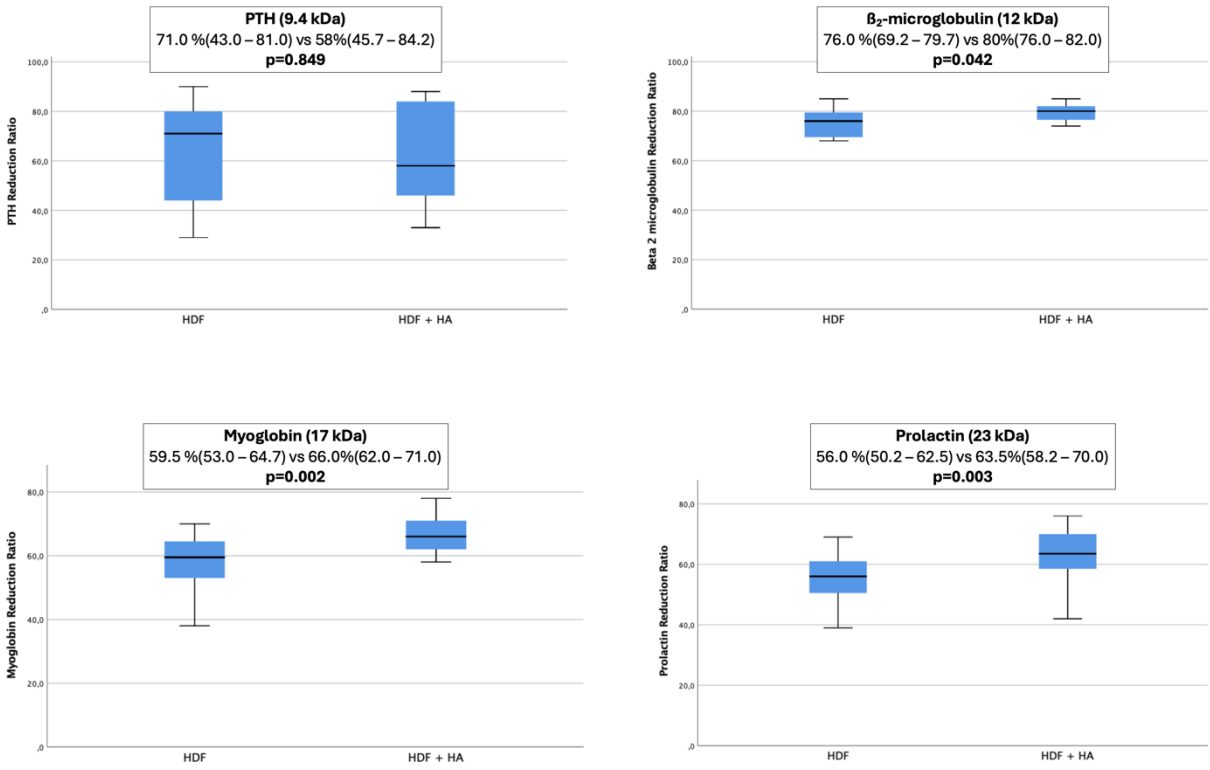

Figure 5.3. Comparison of reduction ratio of four middle molecules. *From the four molecules studied, only PTH had a similar reduction ration in HDF + HA or in HA. For dß$_2$-microglobulin, myoglobin and prolactin the reduction ratio was higher in HDF + HA. HA, hemoadsorption; HDF, hemodiafiltration.*

Discussion

Recently, Maduell and co-workers(57) carried out a prospective study where patients performed HAHDF and HDF. There was only a modest increment in the RR of the same middle molecules explored in our study, not reaching statistical significance. In contrast, we consistently found gains in the removal of molecules with molecular weight ≥12 kDa. One of the reasons for the different results might be that in Maduell's study, the patients carried out 5-hour session, while in ours, the session duration was 3 hours. Perhaps after three hours, the cartridge is saturated and the gains in removal during the first 3 hours might dissipate in the next two hours of the session. Evidence from studies with hemoadsorption in acute settings demonstrate cartridge saturation before four to six hours for bilirubin(58) (0.58 kDa), and myoglobin(59) (17.0 kDa). Importantly, the mass of styrene-divinylbenzene in these cartridges used in acute setting is three times higher the mass of cartridges for maintenance dialysis patients. Therefore, saturation might occur even earlier than 3 hours of therapy.

Conclusion

A 3-hour session of HAHDF provide superior reduction ratio of three middle molecules when compared to post-filter HDF. Prospective studies comparing clinical outcomes are warranted.

Chapter 6

In Vitro Myoglobin Adsorption in Cartridges with Mesoporous Styrene-Divinylbenzene Resin (ongoing project at the University of São Paulo)

Introduction

Rhabdomyolysis describes the disintegration of skeletal muscle cells, resulting in the release of intracellular components into the circulation(60). The primary etiology is traumatic injury, such as in cases of polytrauma(61). Other causes include sepsis, myotoxicity induced by certain medications, and snakebite incidents(62),(63). In addition to the release of intracellular potassium and phosphate, there is a concomitant release of creatine kinase and myoglobin into the bloodstream. Following muscle injury, myoglobin levels peak at approximately 12 hours and are subsequently cleared by the kidneys. The half-life of myoglobin is approximately 3 hours under normal renal function and in the absence of ongoing muscle injury(64). However, the accumulation of myoglobin can lead to nephrotoxicity, although the cellular mechanisms underlying this renal injury remain to be fully elucidated(65).

Prophylactic measures to prevent acute kidney injury include urine alkalinization,[7] though randomized studies supporting this strategy are lacking(66). In cases of acute kidney injury secondary to rhabdomyolysis, renal replacement therapy with hemodialysis may be necessary. Moreover, hemodialysis and, particularly, hemoadsorption procedures are capable of removing myoglobin, potentially preventing or mitigating renal damage(67). According to current classification,[12] myoglobin is a moderately hydrophilic molecule with an intermediate molecular weight (>15 – 25 kDa), specifically 17 kDa. Due to its physicochemical properties, the clearance of myoglobin using current hemodialysis filters is limited(68).

Notably, the removal of myoglobin is enhanced through the use of hemoadsorption cartridges containing polystyrene-divinylbenzene sorbents. Clinical evidence demonstrates that this approach can achieve removal comparable to or exceeding that of conventional hemodialysis(69). There is clinical interest in exploring the kinetics of adsorption-based clearance to define adsorption isotherms at body temperature and the

maximum adsorptive capacity of the sorbent for myoglobin molecules. Previously, our research group has investigated the adsorption kinetics of antimicrobials, iodinated contrast and bilirubin in in vitro closed-circuit models(12),(28),(31),(70). The objective of this study is to evaluate the adsorptive capacity of myoglobin using a cartridge containing polystyrene-divinylbenzene resin in a closed circuit designed to simulate an extracorporeal blood purification system.

Materials and Methods

The primary outcome of your experiment is to evaluate the efficacy of cartridges containing polystyrene-divinylbenzene sorbent in the adsorption of myoglobin from a simulated blood circulation solution. Secondary outcomes include to determine the ratio between the initial myoglobin concentration and the collected concentration at various time intervals within the reservoir, following passage through a closed-loop circuit with an intermediary adsorption resin cartridge. The resulting value, obtained by dividing the myoglobin concentration at a specific time point by the initial concentration, is referred to as the reduction ratio. Additionally, we aim to estimate the total mass of myoglobin that can be adsorbed by the cartridge until saturation, thereby providing a quantitative measure of the sorbent cartridge's total adsorption capacity. Finally, we intend to identify the time point at which the polystyrene-divinylbenzene resin attains its maximum myoglobin adsorption capacity, indicated by the cessation of a progressive decrease in myoglobin concentration within the resevoir which determines the saturation of the resin.

We carried out experiments 1 and 2 without a solution with albumin as the solvent solution because of the elevated costs of this medication. We performed these two experiments in November 2024. We used a simplified version (**Figure 6.1**) of the original GALILEO machine (**Figure 6.2**), equipped with a single peristaltic pump.

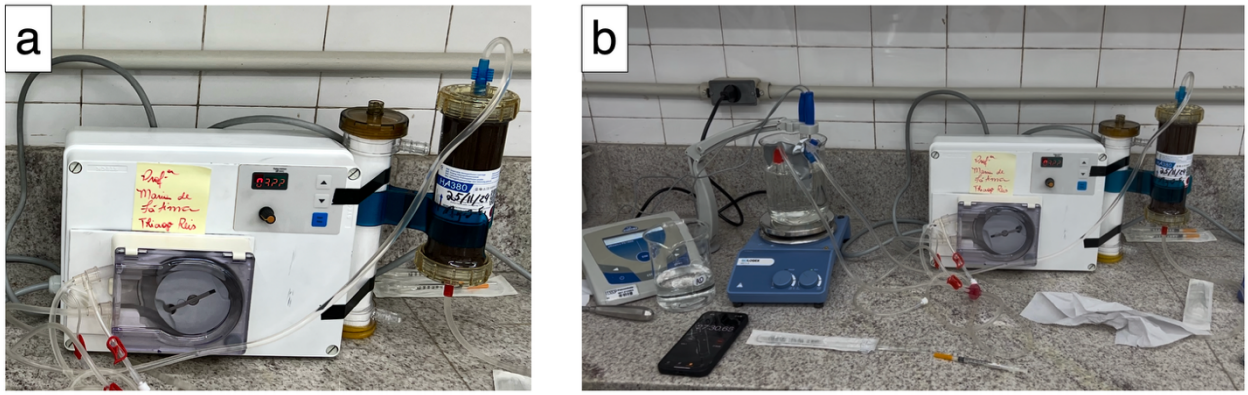

***Figure 6.1. Perfusion machine**. a) An adapted single peristaltic pump device. The filter on the right side of the machine is used solely to support the cartridge's plastic claw. b) Experiment setup.*

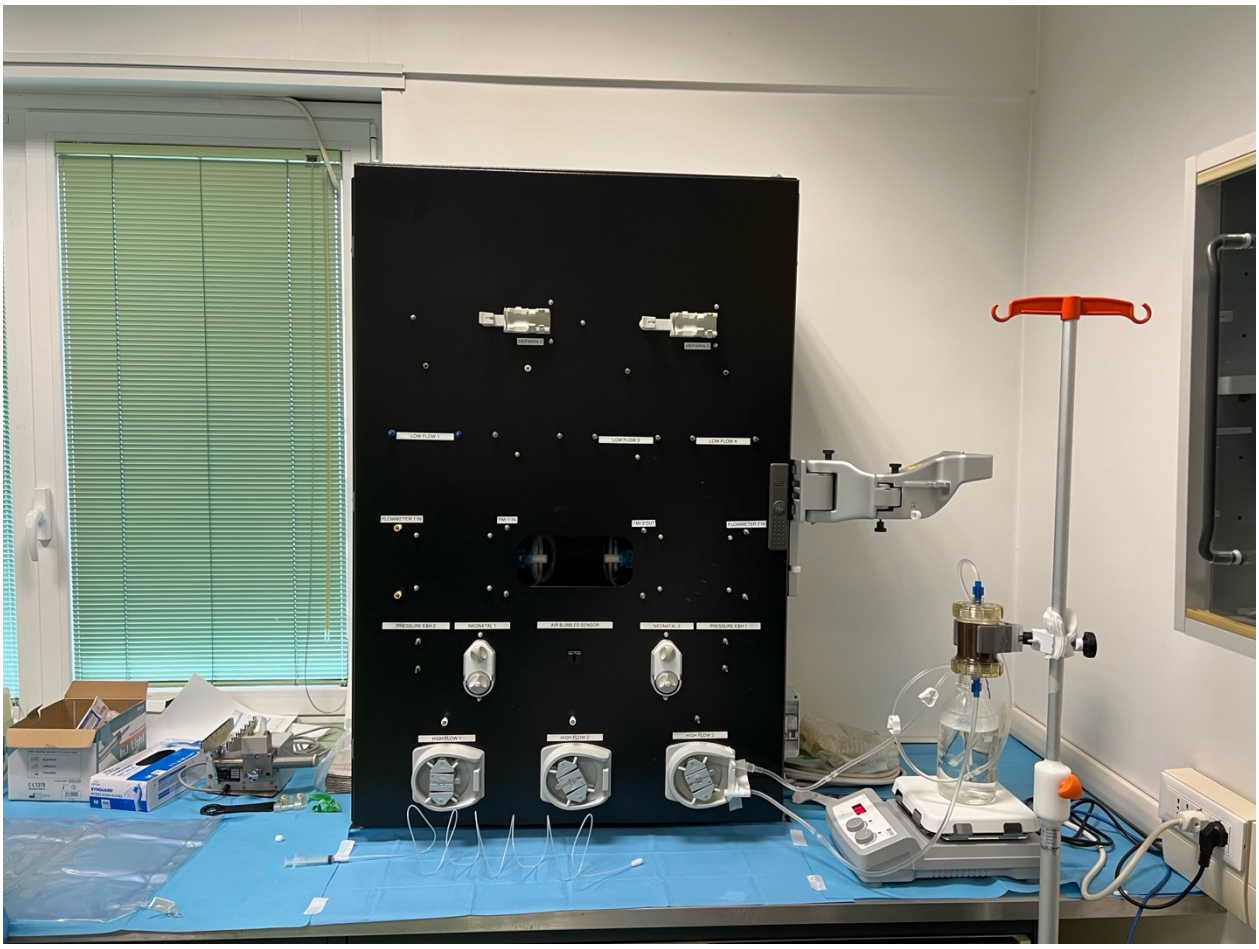

***Figure 6.2. GALILEO machine platform.** This 1.5 m tall metallic box displays three peristaltic pumps used in adult dialysis machines in the bottom, followed by two peristaltic pediatric pumps and two piston pump*

syringes at the top. This machine is located at the Laboratory of Bioengineering at International Renal Research Institute of Vicenza.

Our main goal is the evaluate the impact of two different flows, that is, 300 mL/min or 100 mL/min. We have chosen these flows because the first is usually used in machines for intermittent hemodialysis and the latter in continuous renal replacement therapy. We will explore that in experiments 3, 4, 5, and 6 (**Table 6.1**).

Table 6.1. *Experiment set-up and involved variables.*

Experiment 1: -Blood flow 300 mL/min -Solvent solution (CRRT dialysate) -Resin mass 285 g (HA380)
Experiment 2: -Blood flow 300 mL/min -Solvent solution (CRRT dialysate) -Resin mass 50 g (HA380 mini-module)
Experiment 3: -Blood flow 300 mL/min -Solvent solution (CRRT dialysate) + 3% Albumin -Resin mass 285 g (HA380)
Experiment 4 -Blood flow 300 mL/min -Solvent solution (CRRT dialysate) + 3% Albumin -Resin mass 50 g (HA380 mini-module)
Experiment 5 -Blood flow 100 mL/min -Solvent solution (CRRT dialysate) + 3% Albumin -Resin mass 285 g (HA380)
Experiment 6 -Blood flow 100 mL/min -Solvent solution (CRRT dialysate) + 3% Albumin -Resin mass 50 g (HA380 mini-module)

In **Table 6.2** we describe the procedures applied:

Table 6.2. *Description of the steps.*

Tubbing and machine
•Install the red tubing (inlet line) in the peristaltic pump of the single pump device. •Connect the male luer connector to the inlet female port (inlet port) of the cartridge (HA380) facing downward.

•Connect the male luer connector from the blue tubing (outlet line) to the inlet female part (outlet port) of the cartridge facing upward.
•Prime the circuit with 1,000 mL of NaCl 154 mmol/L (0.9%0 solution at 250 mL/min for 4 minutes. During the priming phase, remove the air/bubbles trapped within the beads by tapping the plastic housing with the rubber hammer.
•Drain completely the circuit.

Solvent solution (30 g/L) human albumin - 1,000 mL

•Fill the glass reservoir with 1000 mL of CRRT fluid, add the magnetic stirring bar.
•Add sodium bicarbonate 8.4% drops until a pH of 7.35 to 7.45 is achieved.
•Place the reservoir on the magnetic stirrer and warm up to 37.0 °C.
•Add 100 mg of myoglobin from equine skeletal muscle (lyophilized powder). Expected final myoglobin concentration of 100,000 ng/mL. Each equine myoglobin bottle has 250 mg (0.250 g).
•Homogenize the solution for a minimum of 5 minutes. If moving particles are still present, wait until the particles are dissolved before starting the experiment.

Priming

•Insert the tip of the inlet line (red) into the reservoir.
•Insert the tip of the outlet line (blue) into the reservoir.
•Start the pump at 300 mL/min. The priming volume considering the tubing and the cartridge is around 160 mL.

Sampling

•Label the syringes and tubes with the timepoint number, minute of sampling and circuit site of sampling. Example: T1, minute 5, pre-cartridge.
•Sampling sites:
a) inlet line (red port plug) defined as pre-cartridge and will be considered also as the reservoir concentration at that timepoint.
b) outlet line (blue port plug) defined as post-cartridge.
• Programmed timepoints (11):

T0 - minute 0; T1 - minute 5; T2 - minute 10; T3 - minute 15; T4 - minute 20; T5 - minute 30; T6 - minute 60; T7 - minute 90; T8 - minute 120; T9 - minute 150; T10 - minute 180; At each timepoint drain 0.4 mL aliquots from each site. •Syringe: 1 mL (aspirate 0.4 mL). •Needle: 0.3 x 8.0 mm •Tube: 1.5 mL microcentrifuge tube with attached lid. Add 0.4 mL of the solution into a labelled microcentrifuge tube.
Pump speed
•For experiment 1, maintain flow speed at 120 mL/min (emulating an continuous renal replacement therapy blood flow). After calibration, to attain 120 mL/min, set to 127 mL/min. •For experiment 2, maintain flow speed at 300 mL/min (emulating a intermittent hemodialysis blood flow). After calibration, to attain 300 mL/min, set to 322 mL/min.

Ethical Considerations

This study was reviewed and approved by the Board of Directors of the Syrian and Lebanese Institute of Research (Project ID No. 3471). In accordance with Resolução 674/2022 - Conselho Nacional de Saúde, Capítulo IX, the project's submission to PLATAFORMA BRASIL and the evaluation by the Ethics Research Committee of the Institution are waived because no human cells or tissues are involved.

Results (preliminary)

In Table 6.3, we describe the results of the initial two experiments. The procedures we uneventful in respect to technical feasibility.

Table 6.3. *Initial results.*

	Experiment 1		Experiment 2	
Time (min)	**Pre (ng/mL)**	**Post (ng/mL)**	**Pre (ng/mL)**	**Post (ng/mL)**
0	57,570	–	32,050	–
5	4,405	1,967	14,730	31,370
10	1,724	1,099	9,952	26,840
15	669	494	16,770	20,920
20	138	50	8,827	5,809
30	1.748	1.172	5,040	3,199
60	0.178	0.091	5,159	14,940
90	0.036	0.022	3,191	3,887
120	0.036	0.0254	13.580	13.080
150	0.030	0.028	9.212	13.950
180	0.025	0.030	7.675	8.242

Discussion

In experiment 1, we had consistency because the post-filter concentrations of myoglobin were lower than the pre-filter concentrations. This was not the case in experiment 2. At this time, we could not explain the issues involved with the conflicting results for experiment 2. Interestingly, a clear visual difference in the translucence of the solution was observed (**Figure 6.3)**

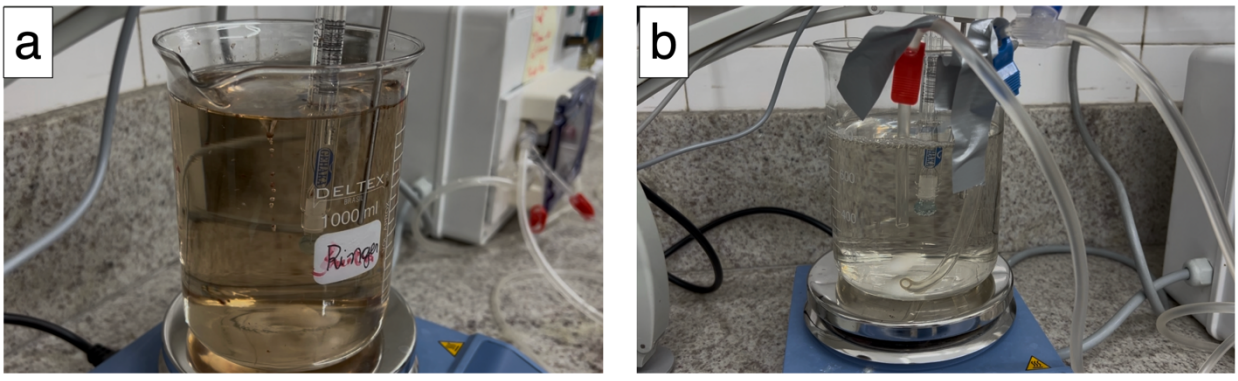

Figure 6.3. Turbidity of the myoglobin solution. *a) before the initiation. b) after 180 minutes.*

Our current hurdle is the dissolution of myoglobin in the CRRT fluid (**Figure 6.4**), because during the experiment these aggregates may continuously release myoglobin, increasing its concentration and underestimating the resin's adsorptive capacity. This aspect was obtained in the solution utilized in the first experiment.

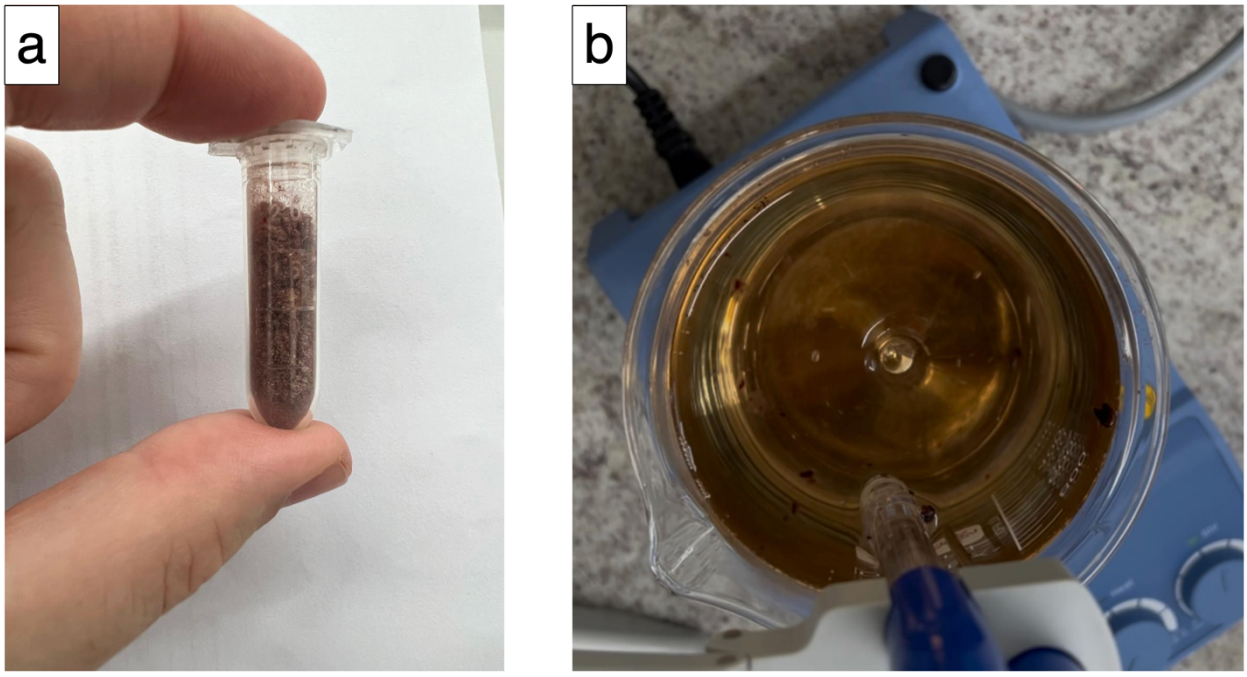

Figure 6.4. Dissolving myoglobin. *a) dehydrated myoglobin powder. b) Top view of a myoglobin solution in a glass reservoir, many dark granules form aggregates of undissolved myoglobin even after 30 minutes of homogenization.*

In experiment number 2, the myoglobin powder was first homogenized in a small reservoir and shaken at high frequency. After visual inspection, no granules were detected in the supernatant; however, some were detected attached to the glass (**Figure 6.5**).

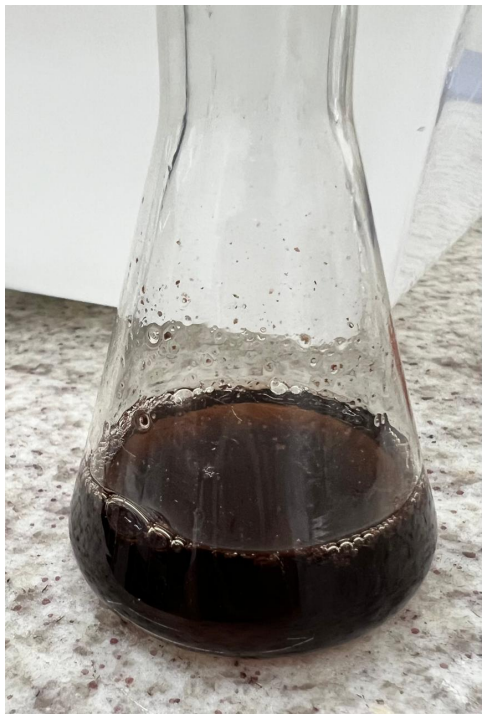

Figure 6.5. Myoglobin solution. *The aspect of the myoglobin powder dissolved in dialysis fluid solution after using the vibrating shaker.*

Closing Remarks

Traditional treatments deployed for extracorporeal blood purification rely on diffusion and convection as elements for mass transport and consequently, blood clearance from a multitude of compounds. The use of adsorption-based modalities with styrene-divinylbenzene resin expands the possibilities for the removal of middle molecules and protein-bound substances. While ongoing research is much needed and constantly refines the understanding of adsorption kinetics and fluid dynamics properties, much evidence has already been established. The investment in basic research is crucial to propel the improvement of the existing technologies and expansion of the current portfolio of cartridges. The field of extracorporeal blood purification is rapidly evolving; nephrologists and intensivists should be familiarized with the mechanisms and principles of hemoadsorption as these treatments are now being routinely applied.

1.3.1 Referências

References:

1. Ronco C, Bordoni V, Levin NW: Adsorbents: From Basic Structure to Clinical Application [Internet]. In: *Contributions to Nephrology*, edited by Ronco C, La Greca G, pp 158–164, 2002 Available from: https://www.karger.com/Article/FullText/60242 [cited 2023 Feb 21]

2. Bellomo R, Ankawi G, Bagshaw SM, Baldwin I, Basu R, Bottari G, Cantaluppi V, Clark W, De Rosa S, Forni LG, Fuhrman D, Goldstein S, Gomez H, Husain-Syed F, Joannidis M, Kashani K, Lorenzin A, Mehta R, Murray PT, Murugan R, Ostermann M, Pannu N, Premuzic V, Prowle J, Reis T, Rimmelé T, Ronco C, Rosner M, Schneider A, See E, Soranno D, Villa G, Whaley-Connell A, Zarbock A: Hemoadsorption: consensus report of the 30th Acute Disease Quality Initiative workgroup. *Nephrol Dial Transplant* gfae089, 2024

3. Bellomo R, Mehta RL, Forni LG, Zarbock A, Ostermann M, Ronco C, on behalf of the Acute Disease Quality Initiative Hemoadsorption Working Group: Hemoadsorption. *Clin J Am Soc Nephrol* [Internet] 2024 Available from: https://journals.lww.com/10.2215/CJN.0000000000000433 [cited 2024 Apr 28]

4. Swenson H, Stadie NP: Langmuir's Theory of Adsorption: A Centennial Review. *Langmuir* 35: 5409–5426, 2019

5. Ronco C, Bellomo R, Kellum JA, Ricci Z, editors: Critical Care Nephrology - Ferrari F, Clark W, Ronco C. Sorbents: from basic structure to clinical application. Third edition. Philadelphia, PA, Elsevier, Inc.

6. Ricci Z, Romagnoli S, Reis T, Bellomo R, Ronco C: Hemoperfusion in the intensive care unit. *Intensive Care Med* 48: 1397–1408, 2022

7. Rokstad A, Strand B, Espevik T, Mollnes T: Biocompatibility and Biotolerability Assessment of Microspheres Using a Whole Blood Model. *Micro and Nanosystems* 5: 177–185, 2013

8. Reis T, Reis F, Fagundes A, da Hora Passos R, Neves F de AR: Rationale for Adsorption in Extracorporeal Blood Purification. *Contrib Nephrol* 200: 1–11, 2023

9. Sing KSW: Characterization Of Porous Solids: An Introductory Survey [Internet]. In: *Studies in Surface Science and Catalysis*, pp 1–9, 1991 Available from: https://linkinghub.elsevier.com/retrieve/pii/S0167299108613038 [cited 2024 Apr 25]

10. Ronco C, Bellomo R: The Process of Adsorption and Cartridge Design [Internet]. In: *Contributions to Nephrology*, edited by Bellomo R, Ronco C, pp 74–81, 2023 Available from: https://karger.com/doi/10.1159/000529295 [cited 2025 Jan 5]

11. Dee KC, Puleo DA, Bizios R: An introduction to tissue-biomaterial interactions. Hoboken, N.J, Wiley-Liss

12. Reis T, Ronco C, Ramírez-Guerrero G, Marcello M, De Cal M, Neves FAR, Lorenzin A: Adsorption Mass Transfer Zone of Vancomycin in Cartridges With Styrene-Divinylbenzene Sorbent. *ASAIO J* [Internet] 2024 Available from: https://journals.lww.com/10.1097/MAT.0000000000002166 [cited 2024 Feb 19]

13. Walther H -J., Faust SD: Adsorption processes for water treatment. *Acta hydrochim hydrobiol* 16: 572–572, 1988

14. Rosenbaum JL: Resin Hemoperfusion for Acute Drug Intoxication. *Arch Intern Med* 136: 263, 1976

15. Ramírez-Guerrero G, Reis T, Segovia-Hernández B, Aranda F, Verdugo C, Pedreros-Rosales C, Marcello M, León J, Rojas A, Galli F, Ronco C: Efficacy of HA130

Hemoadsorption in Removing Advanced Glycation End Products in Maintenance Hemodialysis Patients. *Artif Organs* aor.14954, 2025

16. Ronco C, Bellomo R: Hemoperfusion: technical aspects and state of the art. *Crit Care* 26: 135, 2022

17. Ronco C, Ghezzi PM, Morris A, Rosales L, Wang E, Zhu F, Metry G, De Simone L, Rhamati S, Adhikarla R, Bashir A, Manzoni C, Spittle M, Levin NW: Blood flow distribution in sorbent beds: analysis of a new sorbent device for hemoperfusion. *Int J Artif Organs* 23: 125–130, 2000

18. Lorenzin A, Neri M, de Cal M, Pajarin G, Mansi Montenegro G, Savastano S, Alghisi A, Ronco C: Fluid Dynamics Analysis by CT Imaging Technique of New Sorbent Cartridges for Extracorporeal Therapies. *Blood Purif* 48: 18–24, 2019

19. Groemer H: Some basic properties of packing and covering constants. *Discrete Comput Geom* 1: 183–193, 1986

20. Polaschegg ND, Ronco C, Soli M: Characterization of Flow-Dynamic Pattern in a New Sorbent Cartridge for Combined Hemoperfusion-Hemodialysis [Internet]. In: *Contributions to Nephrology*, edited by Ronco C, Winchester JF, pp 154–165, 2001 Available from: https://www.karger.com/Article/FullText/60119 [cited 2023 Nov 11]

21. Toye D, Marchot P, Crine M, L'Homme G: Modelling of multiphase flow in packed beds by computer-assisted x-ray tomography. *Meas Sci Technol* 7: 436–443, 1996

22. Dąbrowski A: Adsorption — from theory to practice. *Adv Colloid Interface Sci* 93: 135–224, 2001

23. Rosner MH, Reis T, Husain-Syed F, Vanholder R, Hutchison C, Stenvinkel P, Blankestijn PJ, Cozzolino M, Juillard L, Kashani K, Kaushik M, Kawanishi H, Massy Z, Sirich TL, Zuo L, Ronco C: Classification of Uremic Toxins and Their Role in Kidney Failure. *Clin J Am Soc Nephrol* 16: 1918–1928, 2021

24. Rybak MJ, Le J, Lodise TP, Levine DP, Bradley JS, Liu C, Mueller BA, Pai MP, Wong-Beringer A, Rotschafer JC, Rodvold KA, Maples HD, Lomaestro BM: Therapeutic monitoring of vancomycin for serious methicillin-resistant *Staphylococcus aureus* infections: A revised consensus guideline and review by the American Society of Health-System Pharmacists, the Infectious Diseases Society of America, the Pediatric Infectious Diseases Society, and the Society of Infectious Diseases Pharmacists. *Am J Health Syst Pharm* 77: 835–864, 2020

25. Lodise TP, Drusano G: Vancomycin Area Under the Curve–Guided Dosing and Monitoring for Adult and Pediatric Patients With Suspected or Documented Serious Methicillin-Resistant *Staphylococcus aureus* Infections: Putting the Safety of Our Patients First. *Clin Infect Dis* 72: 1497–1501, 2021

26. Pai MP, Neely M, Rodvold KA, Lodise TP: Innovative approaches to optimizing the delivery of vancomycin in individual patients. *Adv Drug Deliv Rev* 77: 50–57, 2014

27. Furukawa T, Lankadeva Y, Baldwin IC, Ow PCC, Hood S, May C, Bellomo R: Vancomycin and Gentamicin Removal with the HA380 Cartridge during Experimental Hemoadsorption. *Blood Purif* 1–8, 2023

28. Ramírez-Guerrero G, Reis T, Lorenzin A, Marcello M, De Cal M, Zanella M, Ronco C: Effect of Mechanical Vibration on Kinetics of Solute Adsorption. *Blood Purif* [Internet] 2024 Available from: https://karger.com/doi/10.1159/000536412 [cited 2024 Feb 19]

29. Lutsenko V, Yelisieiev V, Sovit Y: Influence of low-frequency vibrations on mass transfer in pores. *Earth Environ Sci* 970: 012020, 2022

30. Eesa M, Barigou M: Enhancing radial temperature uniformity and boundary layer development in viscous Newtonian and non-Newtonian flow by transverse oscillations: A CFD study. *Chemical Engineering Science* 65: 2199–2212, 2010

31. Reis T, Ramírez-Guerrero G, Pecoits-Filho R, Lorenzin A, De Cal M, Corradi V, Klinkmann G, Ronco F, Neves FAR, Bellomo R, Ronco C: Iodinated Contrast Adsorption in Cartridges With Styrene-Divinylbenzene Sorbent. *Artif Organs* 49: 813–819, 2025

32. Mehta R, Sorbo D, Ronco F, Ronco C: Key Considerations regarding the Renal Risks of Iodinated Contrast Media: The Nephrologist's Role. *Cardiorenal Med* 13: 324–331, 2023

33. Stevens PE, Ahmed SB, Carrero JJ, Foster B, Francis A, Hall RK, Herrington WG, Hill G, Inker LA, Kazancıoğlu R, Lamb E, Lin P, Madero M, McIntyre N, Morrow K, Roberts G, Sabanayagam D, Schaeffner E, Shlipak M, Shroff R, Tangri N, Thanachayanont T, Ulasi I, Wong G, Yang C-W, Zhang L, Levin A: KDIGO 2024 Clinical Practice Guideline for the Evaluation and Management of Chronic Kidney Disease. *Kidney Int* 105: S117–S314, 2024

34. Roscigno G, Quintavalle C, Biondi-Zoccai G, De Micco F, Frati G, Affinito A, Nuzzo S, Condorelli G, Briguori C: Urinary Dickkopf-3 and Contrast-Associated Kidney Damage. *J Am Coll Cardiol* 77: 2667–2676, 2021

35. Jensen SK, Heide-Jørgensen U, Gammelager H, Birn H, Christiansen CF: Acute Kidney Injury Duration and 20-Year Risks of CKD and Cardiovascular Disease. *Kidney Int Rep* 9: 817–829, 2024

36. Cheng W, Wu X, Liu Q, Wang H-S, Zhang N-Y, Xiao Y-Q, Yan P, Li X-W, Duan X-J, Peng J-C, Feng S, Duan S-B: Post-contrast acute kidney injury in a hospitalized population: short-, mid-, and long-term outcome and risk factors for adverse events. *Eur Radiol* 30: 3516–3527, 2020

37. Li Y, Wang J: Contrast-induced acute kidney injury: a review of definition, pathogenesis, risk factors, prevention and treatment. *BMC Nephrol* 25: 140, 2024

38. Cashion W, Weisbord SD: Radiographic Contrast Media and the Kidney. *Clin J Am Soc Nephrol* 17: 1234–1242, 2022

39. Angheloiu GO, Hänscheid H, Wen X, Capponi V, Anderson WD, Kellum JA: Experimental First-Pass Method for Testing and Comparing Sorbent Polymers Used in the Clearance of Iodine Contrast Materials. *Blood Purif* 34: 34–39, 2012

40. Angheloiu GO, Hänscheid H, Reiners C, Anderson WD, Kellum JA: In vitro catheter and sorbent-based method for clearance of radiocontrast material during cerebral interventions. *Cardiovasc Revasc Med* 14: 207–212, 2013

41. Gualano SK, Seth M, Gurm HS, Sukul D, Chetcuti SJ, Patel HJ, Merhi W, Schwartz C, O'Neill WW, Shannon F, Grossman PM: Renal Function–Based Contrast Threshold Predicts Kidney Injury in Transcatheter Aortic Valve Replacement. *JSCAI* 1: 100038, 2022

42. Amin AP, Bach RG, Caruso ML, Kennedy KF, Spertus JA: Association of Variation in Contrast Volume With Acute Kidney Injury in Patients Undergoing Percutaneous Coronary Intervention. *JAMA Cardiol* 2: 1007, 2017

43. Soman RS, Zahir H, Akhlaghi F: Development and validation of an HPLC-UV method for determination of iohexol in human plasma. *J Chromatogr B Analyt Technol Biomed Life Sci* 816: 339–343, 2005

44. Davidson LJ, Davidson CJ: Acute Kidney Injury and TAVR: Time to Turn Down the (Contrast) Volume. *J Soc Cardiovasc Angiogr Interv* 1: 100310, 2022

45. Reis T, Ramos De Freitas GR, Reis F, Cascelli De Azevedo ML, Dias P, Figueiredo Santos DF, Vivanco Vergara RA, Sgarabotto L, Reis Da Silva Filho E, Ronco C: Regional Hypertonic Citrate Anticoagulation in Membrane Therapeutic Plasma Exchange: A Case Series. *Can J Kidney Health Dis* 8: 205435812110547, 2021

46. Ramírez-Guerrero G, Reis T, Segovia-Hernández B, Aranda F, Verdugo C, Pedreros-Rosales C, Marcello M, León J, Rojas A, Galli F, Ronco C: Efficacy of HA130 Hemoadsorption in Removing Advanced Glycation End Products in Maintenance Hemodialysis Patients. *Artif Organs* 49: 900–906, 2025

47. Clark WR, Dehghani NL, Narsimhan V, Ronco C: Uremic Toxins and their Relation to Dialysis Efficacy. *Blood Purif* 48: 299–314, 2019

48. Reis T, Hutchison C, De Assis Rocha Neves F, Zawadzki B, Zanella M, Ronco C, Rosner MH: Rationale for a New Classification of Solutes of Interest in Chronic Kidney Disease and Hemodialysis. *Blood Purif* 52: 242–254, 2023

49. Stinghen AEM, Massy ZA, Vlassara H, Striker GE, Boullier A: Uremic Toxicity of Advanced Glycation End Products in CKD. *J Am Soc Nephrol* 27: 354–370, 2016

50. Gerdemann A: Plasma levels of advanced glycation end products during haemodialysis, haemodiafiltration and haemofiltration: potential importance of dialysate quality. *Nephrol Dial Transplant* 17: 1045–1049, 2002

51. Ankawi G, Fan W, Pomarè Montin D, Lorenzin A, Neri M, Caprara C, de Cal M, Ronco C: A New Series of Sorbent Devices for Multiple Clinical Purposes: Current Evidence and Future Directions. *Blood Purif* 47: 94–100, 2019

52. Zhang Y, Mei C-L, Rong S, Liu Y-Y, Xiao G-Q, Shao Y-H, Kong Y-Z: Effect of the Combination of Hemodialysis and Hemoperfusion on Clearing Advanced Glycation End Products: A Prospective, Randomized, Two-Stage Crossover Trial in Patients Under Maintenance Hemodialysis. *Blood Purif* 40: 127–132, 2015

53. Raucci A, Cugusi S, Antonelli A, Barabino SM, Monti L, Bierhaus A, Reiss K, Saftig P, Bianchi ME: A soluble form of the receptor for advanced glycation endproducts (RAGE) is produced by proteolytic cleavage of the membrane-bound form by the sheddase a disintegrin and metalloprotease 10 (ADAM10). *FASEB j* 22: 3716–3727, 2008

54. Reis T, Guimaraes MG, Pecoits-Filho R, Andrade J, Braga S, MacIel GG, Goes M, Kitawara K, Ramírez-Guerrero G, Neves F, Ronco C, Noronha IL: Removal of middle molecules with hemoadsorption plus hemodiafiltration in kidney failure patients. *Nephrology Dialysis Transplantation* 40: gfaf116.0655, 2025

55. Maduell F, Broseta JJ, Rodas L, Montagud-Marrahi E, Rodriguez-Espinosa D, Hermida E, Arias-Guillén M, Fontseré N, Vera M, Gómez M, González B, Rico N: Comparison of Solute Removal Properties Between High-Efficient Dialysis Modalities in Low Blood Flow Rate. *Ther Apher Dial* 24: 387–392, 2020

56. Maduell F, Broseta JJ, Rodríguez-Espinosa D, del Risco J, Rodas LM, Arias-Guillén M, Vera M, Fontseré N, Salgado M del C, Rico N: Comparison of four medium cut-off dialyzers. *Clin Kidney J* 15: 2292–2299, 2022

57. Maduell F, Escudero-Saiz VJ, Cuadrado-Payán E, Rodriguez-Garcia M, Rodas LM, Fontseré N, Salgado MDC, Casals G, Rico N, Broseta JJ: Comparing hemodialysis and hemodiafiltration performance with and without hemoadsorption. *Clin Kidney J* 18: sfaf146, 2025

58. Greimel A, Habler K, Gräfe C, Maciuga N, Brozat CI, Vogeser M, Zoller M, Happich FL, Liebchen U, Frank S, Paal M, Scharf C: Extracorporeal adsorption of protective and toxic bile acids and bilirubin in patients with cholestatic liver dysfunction: a prospective study. *Ann Intensive Care* 13: 110, 2023

59. Graf H, Gräfe C, Bruegel M, Zoller M, Maciuga N, Frank S, Weidhase L, Paal M, Scharf C: Myoglobin adsorption and saturation kinetics of the cytokine adsorber Cytosorb® in patients with severe rhabdomyolysis: a prospective trial. *Ann Intensive Care* 14: 96, 2024

60. Ramírez-Guerrero G, Reis T, Marcello M, De Cal M, Ronco C: Crush syndrome-related acute kidney injury in earthquake victims, time to consider new therapeutical options? *Int J Artif Organs* 47: 3–7, 2024

61. Edouard P, Reurink G, Mackey AL, Lieber RL, Pizzari T, Järvinen TAH, Gronwald T, Hollander K: Traumatic muscle injury. *Nat Rev Dis Primers* 9: 56, 2023

62. Gutiérrez JM, Calvete JJ, Habib AG, Harrison RA, Williams DJ, Warrell DA: Snakebite envenoming. *Nat Rev Dis Primers* 3: 17063, 2017

63. Kolovou G, Cokkinos P, Bilianou H, Kolovou V, Katsiki N, Mavrogeni S: Non-traumatic and non-drug-induced rhabdomyolysis. *Arch Med Sci Atheroscler Dis* 4: 252–263, 2019

64. Holt S, Moore K: Pathogenesis of Renal Failure in Rhabdomyolysis: The Role of Myoglobin. *Nephron Exp Nephrol* 8: 72–76, 2000

65. Messerer DAC, Halbgebauer R, Nilsson B, Pavenstädt H, Radermacher P, Huber-Lang M: Immunopathophysiology of trauma-related acute kidney injury. *Nat Rev Nephrol* 17: 91–111, 2021

66. Kodadek L, Carmichael SP, Seshadri A, Pathak A, Hoth J, Appelbaum R, Michetti CP, Gonzalez RP: Rhabdomyolysis: an American Association for the Surgery of Trauma Critical Care Committee Clinical Consensus Document. *Trauma Surg Acute Care Open* 7: e000836, 2022

67. Jerman A, Andonova M, Persic V, Gubensek J: Extracorporeal Removal of Myoglobin in Patients with Rhabdomyolysis and Acute Kidney Injury: Comparison of High and Medium Cut-Off Membrane and an Adsorber Cartridge. *Blood Purif* 51: 907–911, 2022

68. Weidhase L, Haussig E, Haussig S, Kaiser T, de Fallois J, Petros S: Middle molecule clearance with high cut-off dialyzer versus high-flux dialyzer using continuous veno-venous hemodialysis with regional citrate anticoagulation: A prospective randomized controlled trial. *PLoS ONE* 14: e0215823, 2019

69. Forni L, Aucella F, Bottari G, Büttner S, Cantaluppi V, Fries D, Kielstein J, Kindgen-Milles D, Krenn C, Kribben A, Meiser A, Mitzner S, Ostermann M, Premuzic V, Rolfes C, Scharf C, Schunk S, Molnar Z, Zarbock A: Hemoadsorption therapy for myoglobin removal in rhabdomyolysis: consensus of the hemoadsorption in rhabdomyolysis task force. *BMC Nephrol* [Internet] 25: 2024 Available from:

https://bmcnephrol.biomedcentral.com/articles/10.1186/s12882-024-03679-8 [cited 2025 July 21]

70. Marcello M, Lorenzin A, De Cal M, Zorzi M, La Malfa MS, Fin V, Sandini A, Fiorin F, Bellomo R, De Rosa S, Ronco C, Zanella M: Bilirubin Removal by Plasmafiltration-Adsorption: Ex vivo Adsorption Kinetics Model and Single Case Report. *Blood Purif* 52: 345–351, 2023

1.3.2 Apêndice

APÊNDICE A – PUBLICAÇÕES DE REVISÃO DO DOUTORANDO A RESPEITO DA TEMÁTICA DA TESE

	Referência		**Citações***
1	Ronco C, Reis T. Continuous renal replacement therapy and extended indications. *Semin Dial*. 2021;34(6):550-560. doi:10.1111/sdi.12963	 REVIEW ARTICLE Seminars in Dialysis WILEY Continuous renal replacement therapy and extended indications Claudio Ronco | Thiago Reis	42
2	Rosner MH, Reis T, Husain-Syed F, et al. Classification of Uremic Toxins and Their Role in Kidney Failure. *Clin J Am Soc Nephrol*. 2021;16(12):1918-1928. doi:10.2215/CJN.02660221	 REVIEW Classification of Uremic Toxins and Their Role in Kidney Failure	230
3	Ricci Z, Romagnoli S, Reis T, Bellomo R, Ronco C. Hemoperfusion in the intensive care unit. *Intensive Care Med*. 2022;48(10):1397-1408. doi:10.1007/s00134-022-06810-1	 Intensive Care Med https://doi.org/10.1007/s00134-022-06810-1 NARRATIVE REVIEW Hemoperfusion in the intensive care unit	106

4	**Reis T, Hutchison C, de Assis Rocha Neves F, et al. Rationale for a New Classification of Solutes of Interest in Chronic Kidney Disease and Hemodialysis. *Blood Purif*. 2023;52(3):242-254. doi:10.1159/000528983**	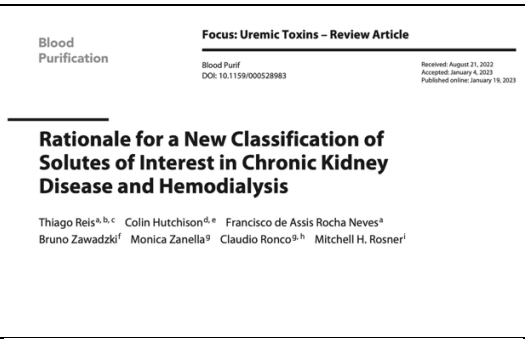 Blood Purification Focus: Uremic Toxins – Review Article Blood Purif DOI: 10.1159/000528983 Received: August 21, 2022 Accepted: January 4, 2023 Published online: January 19, 2023 **Rationale for a New Classification of Solutes of Interest in Chronic Kidney Disease and Hemodialysis** Thiago Reis[a, b, c] Colin Hutchison[d, e] Francisco de Assis Rocha Neves[a] Bruno Zawadzki[f] Monica Zanella[g] Claudio Ronco[g, h] Mitchell H. Rosner[i]	15
5	**Reis T, Reis F, Fagundes A Jr, da Hora Passos R, Neves FAR. Rationale for Adsorption in Extracorporeal Blood Purification. *Contrib Nephrol*. 2023;200:107-117. doi:10.1159/000527707**	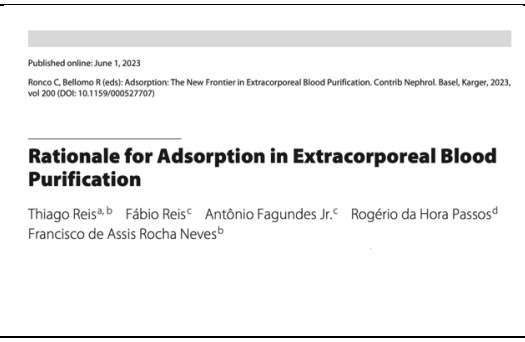 Published online: June 1, 2023 Ronco C, Bellomo R (eds): Adsorption: The New Frontier in Extracorporeal Blood Purification. Contrib Nephrol. Basel, Karger, 2023, vol 200 (DOI: 10.1159/000527707) **Rationale for Adsorption in Extracorporeal Blood Purification** Thiago Reis[a, b] Fábio Reis[c] Antônio Fagundes Jr.[c] Rogério da Hora Passos[d] Francisco de Assis Rocha Neves[b]	7
6	Ramírez-Guerrero G, Ronco C, Reis T. Chronic Kidney Disease-Associated Pruritus: Nomenclature and Treatment - We Need to Take Two Steps Forward. *Blood Purif*. 2023;52(9-10):821-823. doi:10.1159/000533469	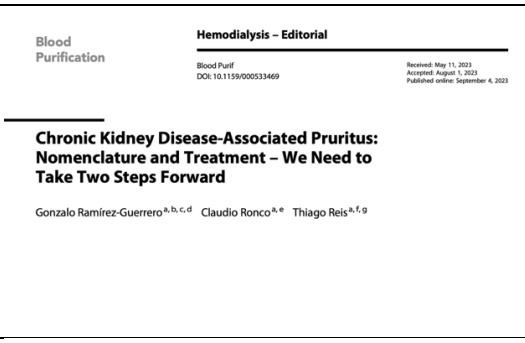 Blood Purification Hemodialysis – Editorial Blood Purif DOI: 10.1159/000533469 Received: May 11, 2023 Accepted: August 1, 2023 Published online: September 4, 2023 **Chronic Kidney Disease-Associated Pruritus: Nomenclature and Treatment – We Need to Take Two Steps Forward** Gonzalo Ramírez-Guerrero[a, b, c, d] Claudio Ronco[a, e] Thiago Reis[a, f, g]	2
7	Ramírez-Guerrero G, Reis T, Marcello M, de Cal M, Ronco C. Crush syndrome-related acute kidney injury in earthquake victims, time to consider new therapeutical options?. *Int J Artif Organs*. 2024;47(1):3-7. doi:10.1177/039139882311 91954	 *Editorial* IJAO The International Journal of Artificial Organs **Crush syndrome-related acute kidney injury in earthquake victims, time to consider new therapeutical options?** The International Journal of Artificial Organs 1–5 © The Author(s) 2023 Article reuse guidelines: sagepub.com/journals-permissions DOI: 10.1177/03913988231191954 journals.sagepub.com/home/jao Sage Gonzalo Ramírez-Guerrero[1,2,3], Thiago Reis[4,5], Matteo Marcello[4], Massimo de Cal[4] and Claudio Ronco[4]	9
8	**Reis T, Ronco C, Soranno DE, et al. Standardization of Nomenclature for the Mechanisms and Materials Utilized for Extracorporeal Blood Purification. *Blood Purif*. 2024;53(5):329-342. doi:10.1159/000533330**	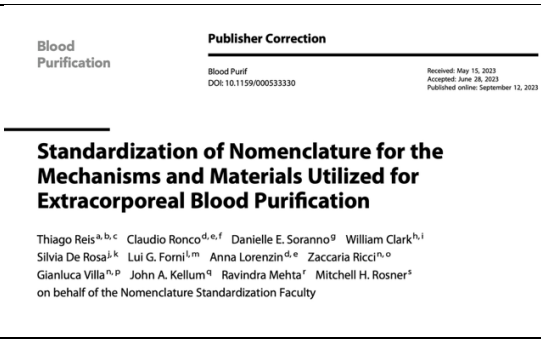 Blood Purification Publisher Correction Blood Purif DOI: 10.1159/000533330 Received: May 15, 2023 Accepted: June 28, 2023 Published online: September 12, 2023 **Standardization of Nomenclature for the Mechanisms and Materials Utilized for Extracorporeal Blood Purification** Thiago Reis[a, b, c] Claudio Ronco[d, e, f] Danielle E. Soranno[g] William Clark[h, i] Silvia De Rosa[j, k] Lui G. Forni[l, m] Anna Lorenzin[d, e] Zaccaria Ricci[n, o] Gianluca Villa[n, p] John A. Kellum[q] Ravindra Mehta[r] Mitchell H. Rosner[s] on behalf of the Nomenclature Standardization Faculty	12

9	Ostermann M, Ankawi G, Cantaluppi V, et al. Nomenclature of Extracorporeal Blood Purification Therapies for Acute Indications: The Nomenclature Standardization Conference. *Blood Purif*. 2024;53(5):358-372. doi:10.1159/000533468	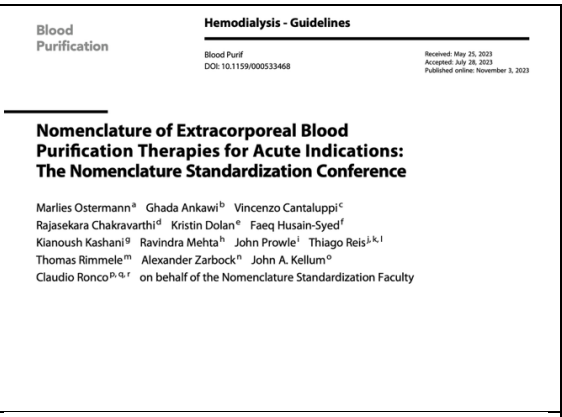	16
10	Ramírez-Guerrero G, Ronco C, Reis T. Cardiorenal Syndrome and Inflammation: A Forgotten Frontier Resolved by Sorbents?. *Cardiorenal Med*. 2024;14(1):454-458. doi:10.1159/000540123		1
11	Zarbock A, Nadim MK, Pickkers P, et al. Sepsis-associated acute kidney injury: consensus report of the 28th Acute Disease Quality Initiative workgroup. *Nat Rev Nephrol*. 2023;19(6):401-417. doi:10.1038/s41581-023-00683-3	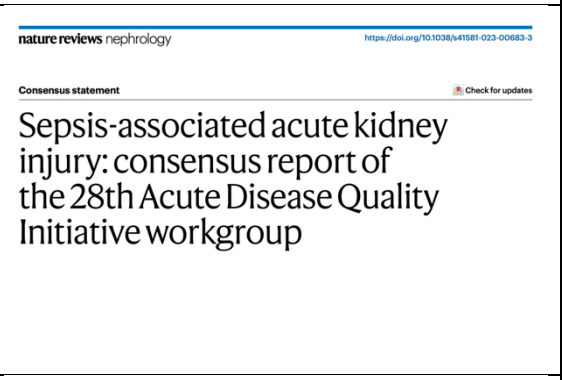	426
12	Bellomo R, Ankawi G, Bagshaw SM, et al. Hemoadsorption: consensus report of the 30th Acute Disease Quality Initiative workgroup. *Nephrol Dial Transplant*. 2024;39(12):1945-1964. doi:10.1093/ndt/gfae089		20